WILEY

Small RNA Mcr11 requires the transcription factor AbmR for stable expression and regulates genes involved in the central metabolism of *Mycobacterium tuberculosis*

Roxie C. Girardin[1] | Kathleen A. McDonough [ID] [1,2]

[1]Department of Biomedical Sciences, School of Public Health, University at Albany, Albany, NY

[2]Wadsworth Center, New York State Department of Health, Albany, NY

Correspondence
Kathleen A. McDonough, Wadsworth Center, New York State Department of Health, 120 New Scotland Avenue, PO Box 22002, Albany, NY 12208.
Email: kathleen.mcdonough@health.ny.gov

Abstract

Mycobacterium tuberculosis (Mtb), the etiologic agent of tuberculosis, must adapt to host-associated environments during infection by modulating gene expression. Small regulatory RNAs (sRNAs) are key regulators of bacterial gene expression, but their roles in Mtb are not well understood. Here, we address the expression and function of the Mtb sRNA Mcr11, which is associated with slow bacterial growth and chronic infections in mice. We found that stable expression of Mcr11 requires multiple factors specific to TB-complex bacteria, including the AbmR transcription factor. Bioinformatic analyses used to predict regulatory targets of Mcr11 identified 7–11 nucleotide regions with potential for direct base-pairing with Mcr11 immediately upstream of Rv3282, *fadA3*, and *lipB*. *mcr11*-dependent regulation of these genes was demonstrated using qRT-PCR and found to be responsive to the presence of fatty acids. Mutation of the putative Mcr11 base-pairing site upstream of *lipB* in a promoter reporter strain resulted in significant de-repression of *lipB* expression, similar to that observed in *mcr11*-deleted Mtb. These studies establish Mcr11's roles in regulating growth and central metabolism in Mtb. Our finding that multiple TB-complex-specific factors are required for production of stable Mcr11 also emphasizes the need to better understand mechanisms of sRNA expression and stability in TB.

KEYWORDS
gene regulation, lipoylation, RNA termination, RNA stability, sRNA targets

1 | INTRODUCTION

Tuberculosis (TB) remains a major threat to global public health, with at least 10 million new, incident cases and 1.3 million deaths due to TB in 2017 (WHO, 2018). The basic biology of *Mycobacterium tuberculosis* (Mtb), the etiological agent of TB, is poorly understood despite its importance to the development of new therapeutic interventions. Mtb can adopt a specialized physiological state within host tissues, which renders the bacteria phenotypically drug resistant and viable despite extended periods of slow or non-replicating persistence (NRP) (Gomez & McKinney, 2004). NRP and phenotypic drug resistance pose particular challenges for intervention, making it critical to understand the regulatory processes that enable Mtb to adapt to host conditions.

Bacterial and host factors that contribute to NRP and slow growth are still being defined (Bergkessel, Basta, & Newman, 2016). Host-associated environmental cues that result in metabolic remodeling and a shift away from active growth toward a state of persistence include

hypoxia, nitrosative stress, redox stress, nutrient starvation, as well as adaptation to cholesterol and fatty acid metabolism (Betts, Lukey, Robb, McAdam, & Duncan, 2002; Garton et al., 2008; Honaker, Dhiman, Narayanasamy, Crick, & Voskuil, 2010; Iona et al., 2016; Schubert et al., 2015; Shi et al., 2005). Lipoylated enzymes involved in the citric acid cycle, such as lipoamide dehydrogenase (Lpd) and dihydrolipoamide acyltransferase (DlaT), are necessary for Mtb survival in the host and viability during NRP (Bryk et al., 2008; Shi & Ehrt, 2006; Venugopal et al., 2011). However, factors that regulate these processes are not well understood.

Gene expression studies have provided critical insights into the regulation and function of proteins like transcription factors that modulate gene expression as Mtb adapts to the host environment during infection (Mvubu, Pillay, Gamieldien, Bishai, & Pillay, 2016; Schnappinger et al., 2003). The additional role of sRNAs in gene regulation is recognized in other bacteria (Waters & Storz, 2009), and several sRNAs whose expression is responsive to stress and/ or growth phase have been identified in mycobacteria (Arnvig et al., 2011; Arnvig & Young, 2009; DiChiara et al., 2010; Gerrick et al., 2018; Miotto et al., 2012; Moores, Riesco, Schwenk, & Arnvig, 2017; Namouchi et al., 2016; Pelly, Bishai, & Lamichhane, 2012; Solans et al., 2014; Tsai et al., 2013). It also has been observed that overexpression of some sRNAs leads to slow or delayed growth in mycobacteria (Arnvig & Young, 2009; Ignatov et al., 2015). Roles for the sRNAs Mcr7, MsrI and 6C/B11 in gene regulation in Mtb or *Mycobacterium smegmati*s (Msm) have been reported (Gerrick et al., 2018; Mai et al., 2019; Solans et al., 2014). However, the importance of these differentially expressed sRNAs to the adaptation and survival of Mtb during periods of stress has not been fully addressed.

The intergenic sRNA Mcr11 (*ncRv11264Ac*) is one of the best-studied mycobacterial sRNAs, but its structure and function in TB-complex mycobacteria is unknown (Arnvig et al., 2011; DiChiara et al., 2010; Girardin, Bai, He, Sui, & McDonough, 2018; Pelly et al., 2012). Expression of Mcr11 is regulated in response to advanced growth phase and levels of the universal second messenger 3′,5′-cyclic adenosine monophosphate (cAMP) (Arnvig et al., 2011; DiChiara et al., 2010; Pelly et al., 2012). Additionally, Mcr11 is abundantly expressed by Mtb in the lungs of chronically infected mice (Pelly et al., 2012) as well as in hypoxic and non-replicating Mtb (Ignatov et al., 2015). Transcriptional regulators of *mcr11* expression include the product of the adjacent, divergently expressed gene *abmR* (Rv1265) (Girardin et al., 2018) and the cAMP-binding transcription factor CRP$_{MT}$ (Arnvig et al., 2011).

Here, we report that cis-acting, extended, native sequence 3′ to Mcr11 enhances transcriptional termination of Mcr11 in mycobacteria. Optimal Mcr11 termination efficiency needed the transcription factor AbmR and was regulated by growth phase in Mtb and *Mycobacterium bovis* BCG, but not in the fast-growing saprophyte *Mycobacterium smegmatis*. We found that *mcr11* regulates expression of *fadA3*, *lipB* and Rv3282, which contribute to central metabolic pathways associated with NRP and slow growth in Mtb. In addition, Mcr11 affected growth of both Mtb and BCG in hypoxic conditions without fatty acids. This study identifies TB complex-specific cis and trans factors required for stable Mcr11 expression while providing a report of *mcr11*-dependent regulation of gene targets in Mtb.

2 | RESULTS

2.1 | Modeling secondary structure of Mcr11

Secondary structural features of sRNAs greatly contribute to their function, and RNA folding is most strongly influenced by the nucleotide sequence of the RNA (Dubey, Baker, Romeo, & Babitzke, 2005; Hnilicova et al., 2014). Previous studies established two 5′ ends of Mcr11 at chromosomal positions 1413224 and 1413227 in *Mycobacterium tuberculosis* H37Rv (Arnvig et al., 2011; DiChiara et al., 2010), but the 3′ end of Mcr11 is poorly defined. Preliminary efforts to express Mcr11 based on size estimates from prior Northern blot experiments were not successful, despite the well-mapped 5′ end of the sRNA. We reasoned that defining the precise boundaries of Mcr11 could help in identifying its function.

We mapped the 3′ end of Mcr11 to chromosomal positions 1413107 and 1413108 in *Mycobacterium tuberculosis* (Mtb) using 3′ rapid amplification of cNDA ends (RACE) and Sanger sequencing (Figure 1a). These 3′ ends are 120 and 119 nucleotides (nt) downstream from the most abundant previously mapped 5′ end at position 1413227 (DiChiara et al., 2010). Our mapped 3′ ends vary 3–4 nucleotides from the 3′ end at chromosomal position 1413111 inferred by deep sequencing (DeJesus et al., 2017), and are 13–14 nt shorter than the 3′ end estimated by cloning (DiChiara et al., 2010) (Figure 1a). These results indicate that Mcr11 is a transcript between 117 and 121 nt long, which is consistent with its observed size by Northern blot (Arnvig et al., 2011; DiChiara et al., 2010; Pelly et al., 2012).

The 3′ ends of Mcr11 varied by 3–14 nt from previous estimates, so we considered the possibility that these variances are functionally significant. Several mycobacterial sRNAs have multiple reported 3′ ends, suggestive of Rho-dependent termination and/or post-transcriptional processing (Arnvig & Young, 2009; Miotto et al., 2012; Tsai et al., 2013). Rho-dependent termination requires the association of the ATP-hydrolyzing molecular motor Rho with the nascent RNA, which is typically cytosine-enriched, guanosine-depleted and unstructured at the 3′ end (Peters et al., 2009). In contrast, intrinsic, Rho-independent termination is governed by the formation of a structured termination hairpin that is usually followed a poly-U tail, and is highly dependent upon the sequence of the nascent RNA (Mooney & Landick, 2013; Ray-Soni, Bellecourt, & Landick, 2016; Santangelo & Artsimovitch, 2011).

We modeled the secondary structure of Mcr11 with varying lengths of extended, native 3′ RNA sequence using RNA structure (Mathews, 2006) to reveal potential functional features. Mcr11 was predicted to be highly structured, with few single-stranded (ss) regions available for potential base-pairing with regulatory target RNA sequences (Figure 1b). Both mapped 5′ ends of *mcr11* produced the same predicted secondary structure, as these 5′ nucleotides are expected to be unpaired (Figure 1b). Modeled structures of extended native sequence

(a)
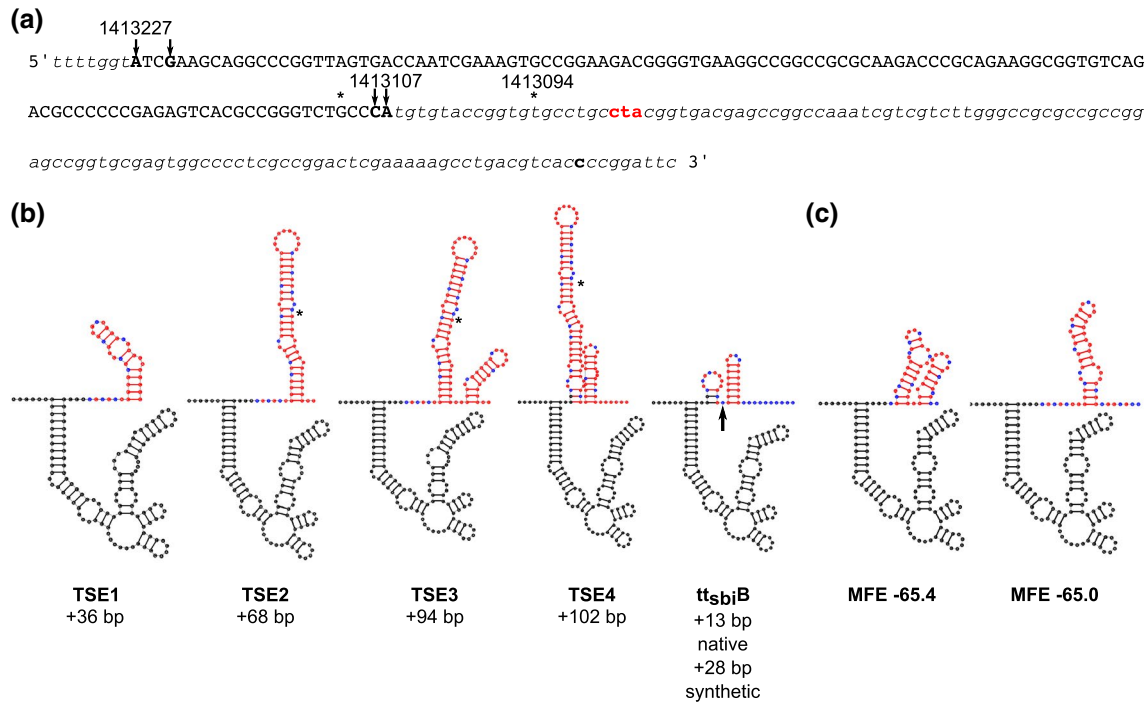
FIGURE 1 Secondary Structure modeling of 3′ sequences beyond the mapped 3′ end of Mcr11. (a) The DNA sequence of the *mcr11* gene and extended 3′ sequence used for modeling experiments is shown. The *mcr11* gene is shown in capital letters, and nucleotides where 5′ and 3′ boundaries have been mapped by RACE are indicated by arrows and shown in capitalized, bolded black text. Flanking sequences are in italics, and the Rv1264 stop codon in bolded red text. The last nucleotide on the 3′ side of mcr11 that was included in modeling experiments is in bold, lowercase black text. An asterisk indicates 3′ ends reported by DiChiara et al and DeJesus et al. Positions of mapped nucleotides on the Mtb chromosome are shown above the text. (b) Secondary structure diagrams of Mcr11 from 5′ position 1413227 and extended 3′ native sequences. The synthetic idealized intrinsic termination control (tt$_{sbi}$B) is also modeled onto Mcr11 from the longest 3′ end reported at position 1413094; the last nucleotide of native sequence 3′ to Mcr11 is indicated by a black arrow. Black nucleotides indicate bases in the mapped boundaries of the *mcr11* gene, red base pairs indicate base pairs beyond the mapped 3′ end of Mcr11 at position 1413107, except all uracils (Us) are shown in blue. An asterisk indicates that last nucleotide modeled in (c). (c). The secondary structure models with the lowest minimum free energies (MFE) of a shorter untested native Mcr11 TSE with the most U rich sequence at the 3′ end of the putative terminator. The MFE of each structure is shown below each diagram [Colour figure can be viewed at wileyonlinelibrary.com]

3′ to our mapped ends of *mcr11* revealed additional highly structured motifs with similarity to predicted Rho-independent terminators (RITs) downstream of *mcr11* in mycobacteria (Gardner, Barquist, Bateman, Nawrocki, & Weinberg, 2011; Mitra, Angamuthu, & Nagaraja, 2008). However, none included the long, characteristic poly-U tail found in RITs of other bacteria (Ray-Soni et al., 2016). A 10 nt region containing a sub-optimal poly-U tract was also identified by scanning sequence downstream of the mapped 3′ end of Mcr11 in the constructs that contained 3′ sequence elements (TSEs) 2–4 (Figure 1a). Modeling the secondary structure of this sequence revealed a potential stem loop structure with a 7nt trail containing four discontinuous Us (Figure 1c).

## 2.2 | Measurement of TSE function in Msm

We tested the impact of different *mcr11* TSEs on the transcriptional termination of Mcr11 using promoter:*mcr11*:TSE:*GFPv* reporter constructs (Figure 2a,b). We reasoned that transcriptional termination levels could be inferred using GFPv fluorescence as a relative measure of transcriptional read-through beyond the *mcr11* gene (Figure 2a). The relative percentage of termination for each

TSE was calculated by dividing the observed fluorescence of each P*mcr11*:TSE:*GFPv* strain by the observed fluorescence of an *mcr11* promoter-only:*GFPv* reporter construct (P*mcr11*:*GFPv*), subtracting the product from 1, and multiplying the result by 100%. Promoterless *GFPv* served as a negative assay control, and an *mcr11*-independent promoter:*GFPv* fusion construct served as a positive assay control. A positive intrinsic termination control was generated by fusing *mcr11* and a small amount of native 3′ trailing sequence to a synthetic RIT (tt$_{sbi}$B) that has been shown to function at ~ 98% efficiency with Mtb RNAP in vitro (Figure 1b) (Czyz, Mooney, Iaconi, & Landick, 2014).

Our initial termination experiments measuring TSE efficiency were performed in Msm, because it lacks an *mcr11* orthologue and thus has no basal Mcr11 expression. The inclusion of any TSE sequence at the 3′ end of *mcr11* resulted in decreased transcriptional read-through of the *mcr11*:GFPv fusion reporter, as compared to the relative levels of GFPv fluorescence for P*mcr11* alone (Figure 2b). This result suggests that all TSEs supported transcriptional termination to varying degrees. TSEs 2–4 had greater termination efficiencies than TSE1, but the positive tt$_{sbi}$B intrinsic termination control exhibited the strongest mean termination efficiency at 88% (Figure 2c). Paraformaldehyde-fixed duplicates of each sample were subjected to flow cytometry analysis to determine

if the mean GFPv fluorescence observed in our plate-based assay was reflective of the fluorescence observed in individual cells, or if there were populations of cells with varying levels of fluorescence. A single, homogenous population of fluorescent cells was observed for each reporter, demonstrating that mean fluorescence measured in the plate reader assay was representative of the fluorescence in individual cells (Supplemental Figure 2). From these data, we concluded that mean fluorescence reflects relative termination efficiency for each TSE reporter.

Northern blot analysis was performed to further evaluate the expression of Mcr11 in Msm. We noted that the size of Mcr11 did not vary in Msm despite the presence of TSEs with various lengths, suggesting that TSEs are rapidly processed of the mature sRNA if they are transcribed (Figure 2d). Larger forms of unprocessed Mcr11 were not observed, but we also noted poor transfer of high molecular weight RNAs (such as rRNA), due to the high percentage of acrylamide in the gel mixture. Mcr11 was also present at very low levels in Msm when compared to a BCG control for which only 1/3 the amount of total RNA present in the Msm samples was loaded in the gel (Figure 2d). These results indicate reduced Mcr11 expression and/or stability in Msm compared to BCG.
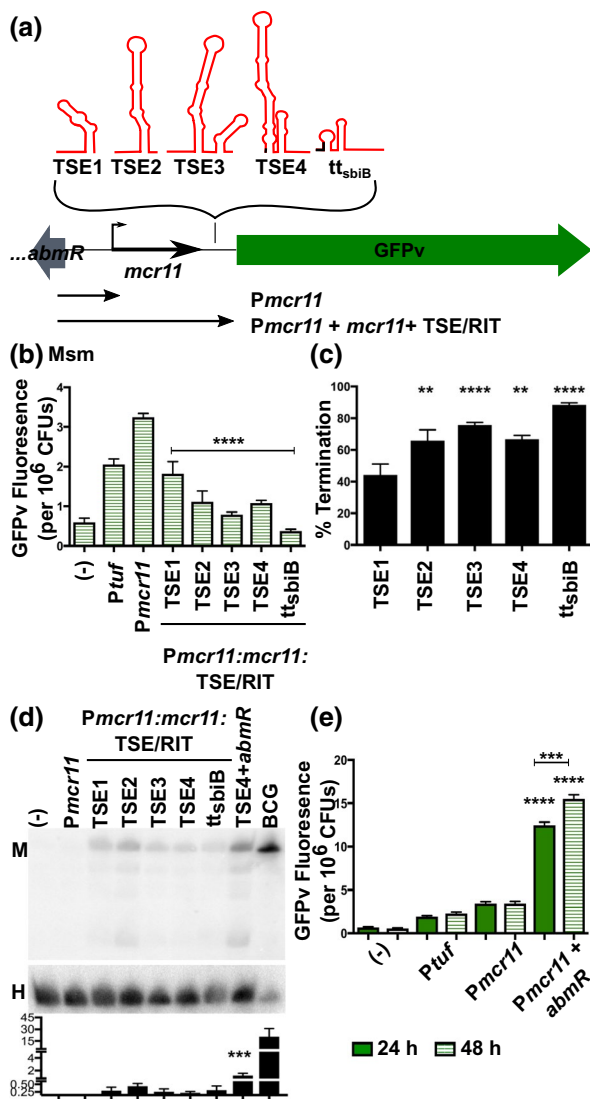
FIGURE 2 TSEs decrease transcriptional read-through of Mcr11-GFPv reporters, but Mcr11 is not robustly expressed in Msm, even in the presence of *abmR* from Mtb. (a). A schematic representation of GFPv fluorescence-based reporter assay to determine the functionality of TSEs, and a synthetic idealized intrinsic termination control (tt$_{sbi}$B). (b). GFPv fluorescence assay used to measure promoter activity and read-through of TSEs of *mcr11* in late stationary phase Msm, which lacks a native *mcr11* locus. The promoter P*tuf* served as a positive control. The various TSE constructs tested are indicated underneath the corresponding bar. Statistical comparisons are relative to P*mcr11*. (c). The % termination of constructs tested in (b). Statistical comparisons are relative to TSE1. (d). Northern blot analysis of Mcr11 expression (M) in Msm with various *mcr11* + TSE constructs. About 10 μg of total Msm RNA was loaded, whereas 3 μg of the BCG positive control was loaded. The HisT tRNA (H) was used as a loading control. The bar chart displays the normalized levels of Mcr11 *as* determined by densitometry. Statistical comparison is between TSE4 + *abmR* and TSEs 1–4 and tt$_{sbiB}$. (e). GFPv fluorescence assay used to measure promoter activity in Msm. Statistical comparisons are relative to P*mcr11* or between 24 h and 28 h as indicated. Fluorescence is normalized to the OD$_{620}$ of each sample. Results are the means of three biological replicates. Statistical analysis conducted with an unpaired, two-tailed Student's *t*-test (e) or by one-way ANOVA with Bonferroni correction for multiple comparisons (b, c, d). Asterisks indicate significance as follows: *p < .05, **p < .01, ***p < .001, ****p < .0001 [Colour figure can be viewed at wileyonlinelibrary.com]

2.3 | TB complex-specific factors are required for stable Mcr11 expression

Mcr11 expression varies across growth phases in TB complex mycobacteria (DiChiara et al., 2010; Girardin et al., 2018), so we examined the effect of growth phase on *mcr11* expression in Msm. Fluorescence from the GFPv transcriptional reporters was measured at mid-log and late stationary phases. Surprisingly, we observed that P*mcr11* activity was not increased by advancing growth phase in Msm (Figure 2e), suggesting lack of a positive regulatory factor.

Previously, we showed that the divergently expressed DNA-binding protein AbmR is a growth phase-responsive activator of *mcr11* expression (Girardin et al., 2018). Although the Msm orthologue (*MSMEG_5010*) of *abmR* displays both high amino acid sequence identity (68.75%) and similarity (83.51%) to AbmR (Girardin et al., 2018), we reasoned that *abmR* could have functionality that the Msm orthologue lacks. Thus, we added a copy of the Mtb *abmR* locus upstream of the P*mcr11:GFPv* fusion sequences and re-tested the activity of P*mcr11* in response to growth phase in Msm. The addition of *abmR* significantly increased P*mcr11* activity in Msm, and rendered P*mcr11* activity responsive to growth phase (Figure 2e), as previously observed in BCG and Mtb (Girardin et al., 2018). Inclusion of *abmR* also significantly increased the amount of stable Mcr11 detected by Northern blot in Msm (Figure 2d), indicating that Mcr11 is unstable even when abundantly transcribed in Msm. Together, these results show that Mtb *abmR* regulates *mcr11* expression at the transcriptional level, but is not sufficient for production of high levels of stable Mcr11 expression in a non-native environment.

Further studies in TB-complex mycobacteria showed that the termination efficiencies of *mcr11* TSEs in mid-log phase BCG

were similar to those observed in Msm (Figure 3), but only BCG showed enhanced *mcr11* TSE termination efficiencies in late stationary phase (Supplemental Table 3A and B). This growth phase-dependent enhancement of termination efficiency in BCG was strongest for TSE1, which increased from approximately 40%–70% (Figure 3c). Overall termination efficiencies of *mcr11* TSEs were also greater in virulent Mtb (H37Rv) than in BCG or Msm (Figure 3d-f). Deletion of *abmR* caused a small but significant decrease in *mcr11* termination efficiencies from all constructs, with the TSE1 short hairpin being the most strongly affected (Supplemental Figure 3).

We used Northern blot analyses to evaluate the size of Mcr11 produced from various *mcr11* TSE constructs in Δ*mcr11* strains of BCG and Mtb during late stationary phase (Figure 4a,b). Robust levels of Mcr11 were produced from constructs containing native *mcr11* TSEs in both BCG and Mtb. As was observed in experiments with Msm, Mcr11 size remained constant despite its expression with TSEs of different

lengths in BCG or Mtb (Figure 4a,b). This size restriction is consistent with precise termination or an RNA processing event that produces discrete 3′ ends. The levels of Mcr11 produced were independent of their TSE in late stationary phase BCG and Mtb, but the Mcr11 constructs produced lower levels in BCG (Figure 4a). Conversely, the levels of Mcr11 generated from Mcr11 constructs in Mtb were more comparable to those observed in the Wt strain (Figure 4b). These data further support the conclusion that species-specific factors have a significant impact on the expression and stability of mature Mcr11.

As advancing growth phase significantly improved the termination efficiencies of TSEs in BCG (Figure 3c), we tested the effects of growth phase on the expression of *mcr11*. We expected that increased termination efficiencies would correlate with higher levels of mature Mcr11 in TB complex mycobacteria. Mcr11 levels were measured by qRT-PCR (Figure 4c) in BCGΔ*mcr11* strains carrying ectopic copies of either *mcr11*:TSE1 or *mcr11*:TSE3. Both constructs
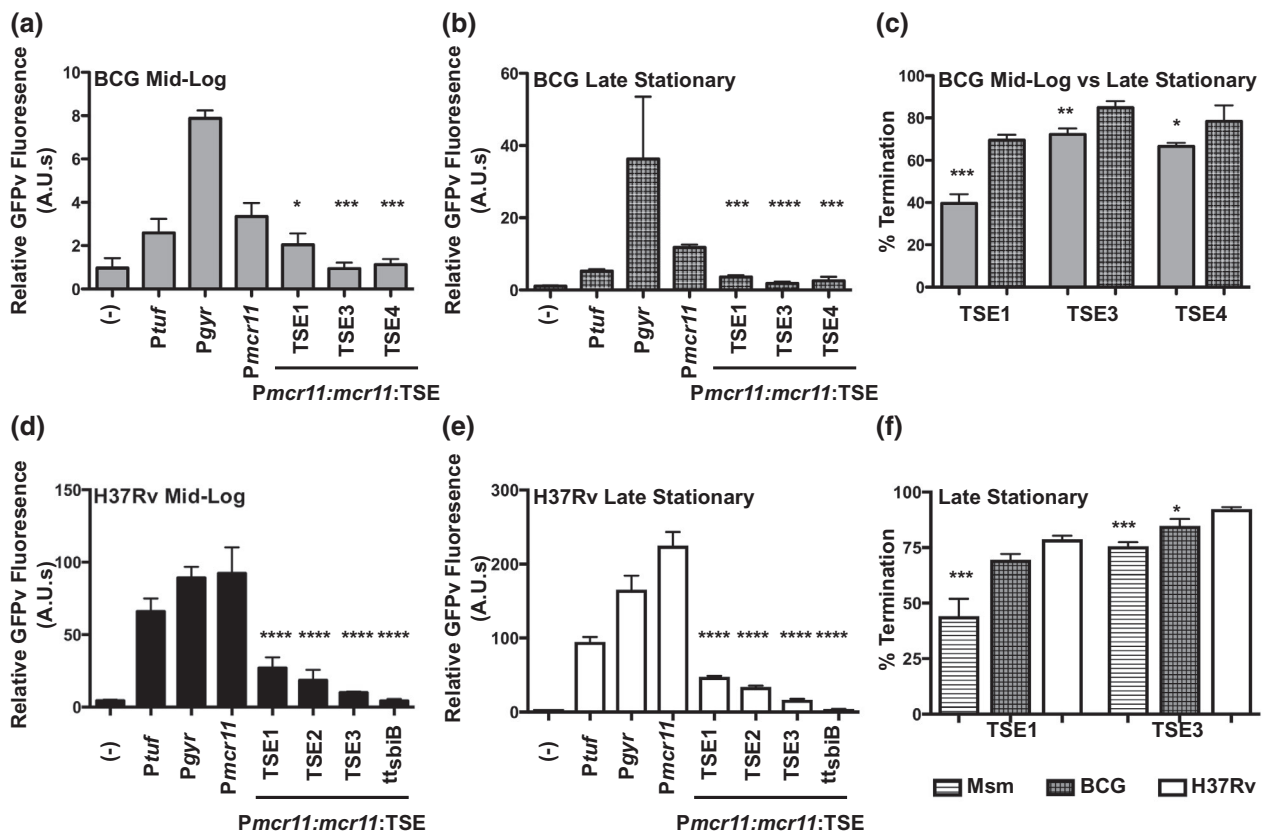
FIGURE 3 Efficiency of TSEs is positively regulated in response to growth phase in BCG and function significantly better in Mtb. (a) GFPv fluorescence assay used to measure promoter activity and read-through of the TSEs of *mcr11* in mid-log phase BCG in hypoxic (1.3% O_2, 5% CO_2), shaking conditions. A promoterless (–) construct was used as a negative control and the promoters P*tuf* and P*gyr* served as positive controls. The various TSE constructs tested are indicated underneath the corresponding bar. Statistical comparisons were made to P*mcr11*. (b) As in (a), but assayed in late stationary phase. (c) A comparison of % termination observed in mid-log phase (solid bars) and late stationary phase (hatched bars) BCG. Statistical comparisons were made between mid-log and stationary phase. (d) GFPv fluorescence assay used to measure promoter activity and read-through of the TSEs of *mcr11* in mid-log phase Mtb in hypoxic (1.3% O_2, 5% CO_2), shaking conditions. A promoterless (–) construct was used as a negative control and the promoters P*tuf* and P*gyr* serve as positive controls. The various TSE constructs tested are indicated underneath the corresponding bar. Statistical comparisons are made to P*mcr11*. Fluorescence is normalized to the OD_{620} of each sample. (e) As in (d), but assayed in late stationary phase. Statistical comparisons are made to P*mcr11*. (f) A comparison of % termination observed in late stationary phase Msm, BCG and Mtb. Statistical comparisons are made to Mtb. Results are the means of three biological replicates. Statistical analysis conducted with a one-way ANOVA with Bonferroni correction for multiple comparisons. Asterisks indicate significance as follows: * $p < .05$, ** $p < .01$, *** $p < .001$, **** $p < .0001$
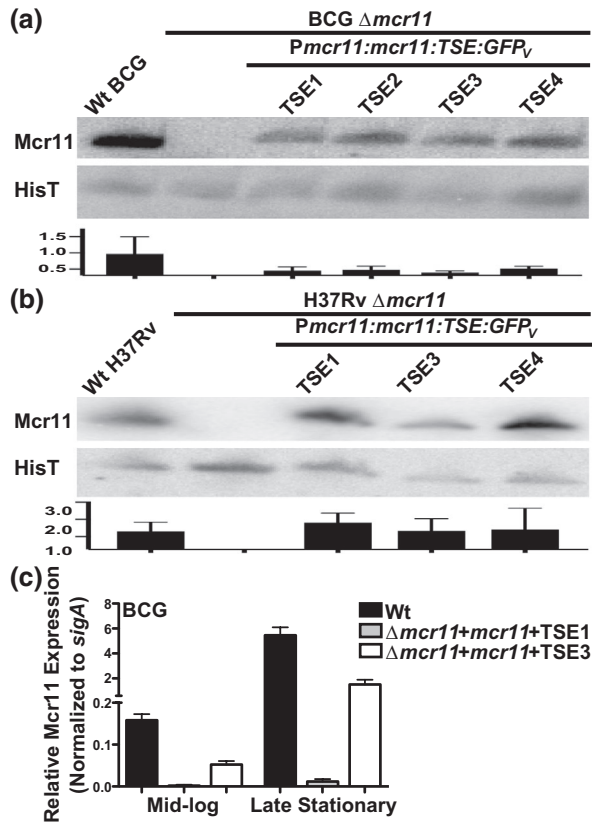
FIGURE 4 Different Mcr11 TSEs do not alter the size of stable Mcr11. Northern blot analysis of Mcr11 expression in (a) BCG or (b) H37Rv in hypoxic (1.3% O_2, 5% CO_2) late stationary phase. The tRNA HisT is used as a loading control. Results of densitometry analysis are presented below the corresponding blot. (c) qPCR analysis of Mcr11 expression in mid-log and late stationary phase BCG, normalized to *sigA* expression. Results representative of 2–3 independent repeats

showed growth phase-dependent increases in expression of stable Mcr11 (Figure 4c). However, the striking increase in Mcr11 produced from TSE3 compared to TSE1 observed by qPCR was not observed by Northern blot analyses of late stationary phase bacteria (Figure 4a). While qPCR has a lower limit of detection than Northern blot analyses, the results suggest that the TSE contributes to the stability of larger, unprocessed transcript products not detected by the Northern blot probe and/or that the secondary structures of the transcripts significantly impact their reverse transcription to cDNA. Together, these data indicate that multiple trans-acting factors specific to the genetic background of TB-complex mycobacteria facilitate the transcriptional termination and production of stable Mcr11.

2.4 | Mcr11 size is unaffected by the presence of a transgene

We considered the possibility that expression of *mcr11* in the context of an mRNA with a translated, stable transgene such as *GFPv* could contribute to the stability or processing of Mcr11. Production

of Mcr11 from *mcr11*:TSE1 constructs was compared to Mcr11 levels from a similar construct in which *GPFv* is not immediately downstream of TSE1 (Supplemental Figure 4). The size of the Mcr11 transcript and Mcr11 levels were unaffected by the GFPv location (Supplemental Figure 4), indicating that *GFPv* did not contribute to the production or processing of stable Mcr11 in these experiments. This conclusion is also consistent with the low levels of Mcr11 observed in Msm despite the presence of the *GFPv* transgene (Figure 2d).

Stress conditions can modulate the efficiency of RITs (Morita, Ueda, Kubo, & Aiba, 2015) and induce the appearance of multiple, different size products of a single sRNA in Mtb (Arnvig & Young, 2009; Namouchi et al., 2016). However, neither BCG nor Mtb displayed significant stress-induced changes in the termination efficiencies of *mcr11* TSEs (Supplemental Table 3) when subjected to nitrosative stress (DETA-NO), ATP depletion (BDQ), DNA damage (OFX), or transcriptional stress (RIF). These data demonstrate that *mcr11* TSEs are not affected by stress.

2.5 | Identification of Mcr11 regulatory targets

Having identified sequence features required for robust ectopic production of Mcr11 in complemented *Δmcr11* strains, we considered *mcr11* function. A bioinformatic search of potential regulatory targets of Mcr11 using TargetRNA (Tjaden, 2008) and TargetRNA2 (Kery, Feldman, Livny, & Tjaden, 2014) identified *abmR* as the top-scoring hit (Figure 5a) (Supplemental Table 4). We measured the relative abundance of AbmR protein by Western blot analysis, and found that it was decreased relative to Wt in BGC*Δmcr11* and Mtb*Δmcr11* (Figure 5b,c). However, recent reports indicate that the *abmR* mRNA is a leaderless transcript that lacks a 5′ UTR (Cortes et al., 2013), so the region of direct base-pair complementarity with the Mcr11 sRNA and the 5′ end of *abmR* predicted by TargetRNA is not likely to be present in the *abmR* mRNA (Cortes et al., 2013). We also previously showed that the *mcr11* gene overlaps a substantial portion of the DNA sequences identified as the upstream enhancer and promoter regions for *abmR* transcription (Figure 5a) (Gazdik, Bai, Wu, & McDonough, 2009; Girardin et al., 2018).

We addressed the possibility that *mcr11* deletion has cis rather than trans effects on *abmR* expression due to disruption of *abmR* regulatory sequences. Promoter:*lacZ* reporter studies were used to compare P*abmR* activity in the presence and absence of flanking *mcr11* sequences in Wt BCG and Mtb backgrounds that express Wt levels of Mcr11. Transcriptional activity from the minimal *abmR* promoter lacking adjacent sequence in the *mcr11* gene was much lower than that from the extended *abmR* promoter that includes contiguous *mcr11* gene sequences (Figure 5d). These assays were conducted in the Wt backgrounds of BCG and Mtb with comparable levels of native *mcr11* expression in all matched strains, indicating that sequence overlapping the *mcr11* gene was required in cis for full *abmR* promoter activity. We conclude that the reduced expression of *abmR* in *Δmcr11* strains is likely due to the loss of cis sequence-based *abmR* regulatory elements within the *mcr11* gene rather than a trans-acting regulatory effect of Mcr11 on *abmR* expression. Additionally,

FIGURE 5 Δ*mcr11* has a disrupted *abmR* promoter, resulting in reduced expression of AbmR protein in BCG and Mtb. (a) The *mcr11* locus with the position of the hygromycin knockout cassette is shown. The regions of DNA used to create *promoter:lacZ* fusions are shown. Fragment (1) includes the *Rv1264-abmR* intergenic region, which includes the *mcr11* locus. Fragment (2) includes the *mcr11-Rv1265* sequence that is available in the Δ*mcr11* strain. (b) Quantification of Western blot analysis from BCG grown to late-log phase in ambient, shaking conditions. (c) Quantification of Western blot analysis from Mtb grown to late-log phase in hypoxic (1.3% O_2, 5% CO_2), shaking conditions. AbmR was detected with poly-clonal anti-sera, and levels were normalized to GlcB levels, as detected by a monoclonal antibody. (d) β-galactosidase activity assays using the promoter:*lacZ* fusions shown in (a) in Wt BCG (gray bars) and MTB (black bars) grown to late-log phase in ambient, shaking conditions. Fluorescence is normalized to the OD_{620} of each sample. An asterisk *indicates *p*-value < .05 using an unpaired Student's *t*-test. Results representative of 2–3 biological repeats
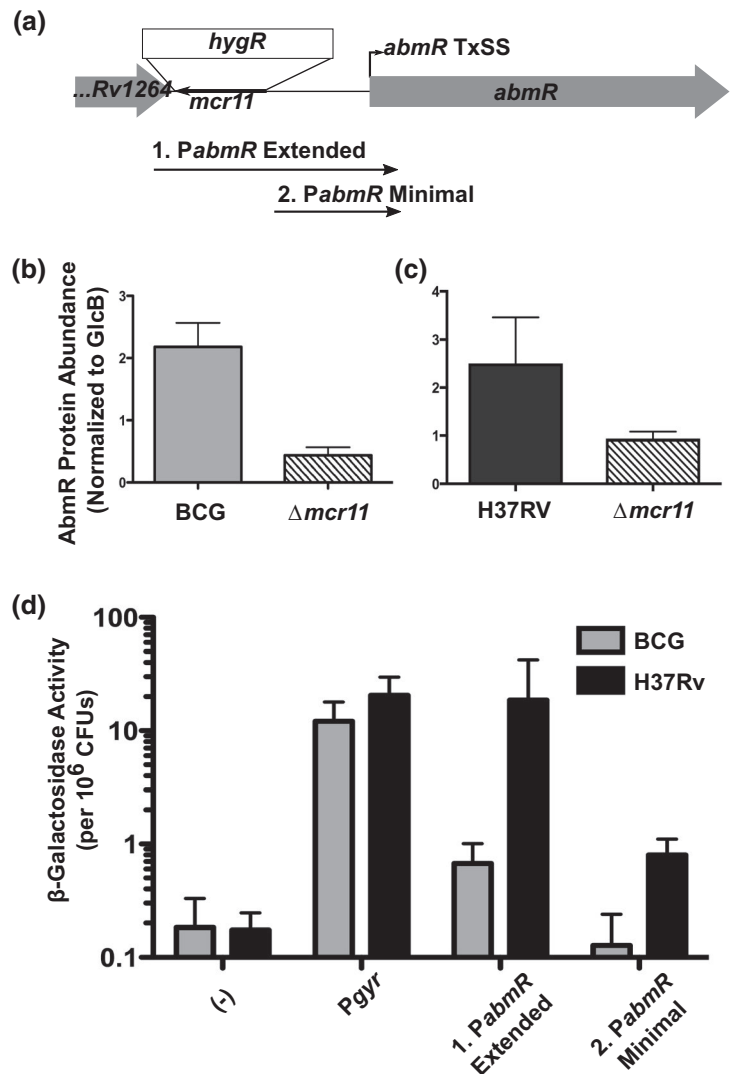

abmR and *mcr11* promoters were both substantially more active in Mtb than in BCG, suggesting that pathogen-specific factors impact the expressivity of both genes.

TargetRNA also predicted multiple putative targets of Mcr11 regulation, including three genes within operons involved in central metabolic processes and cell division: *lipB* (encodes lipoate-protein ligase B, needed for lipoate biosynthesis) (Figure 6a), Rv3282 (encodes a conserved hypothetical protein with homology to Maf septum-site inhibition protein) (Figure 6b) and *fadA3* (encodes a beta-ketoacyl coenzyme A thiolase) (Figure 6c). The intergenic spacing between putative target gene *fadA3* and the preceding gene (Rv1075c) is identical to that of the intergenic spacing between Rv2216 and *lipB* (Figure 6a,c). However, *fadA3* is likely to be transcribed independently of *Rv1075c* (Cortes et al., 2013). *fadA3*, *lipB* and Rv3282 were selected for follow-up because they are associated with growth and central metabolism of Mtb and contain predicted Mcr11 base-pairing sequences that are within known mRNA transcript boundaries. Each of these target transcripts has the potential to interact with Mcr11 through a 7–11 nt continuous base-pairing region adjacent to a shorter stretch of gapped or imperfect

base-pairing (Figure 6a,c). A region from nt 39–55 of Mcr11 that is located within an unpaired loop of multiple modeled secondary structures of Mcr11 (Supplemental Figure 5) was predicted to interact with these mRNA targets (Figure 6d, Supplemental Table 4).

2.6 | Fatty acids affect Mcr11-dependent regulation of target genes in Mtb

The *lipB* operon includes *dlaT*, which encodes DlaT, the E2 component of pyruvate dehydrogenase (PDH) and the peroxynitrite reductase/peroxidase (PNR/P) complex in Mtb. The function of DlaT is modulated by lipoylation, which is dependent upon lipoate biosynthesis by LipB (Spalding & Prigge, 2010; Venugopal et al., 2011). BkdC (also called PdhC or Rv2495c) is a component of the branched chain keto-acid dehydrogenase (BCKADH) complex in Mtb that also requires lipoylation for activity. Disruption of components in any of these complexes can cause growth defects in Mtb, some of which are dependent upon the nutrient mixture present in the growth media (Shi & Ehrt, 2006; Venugopal et al., 2011). The genes
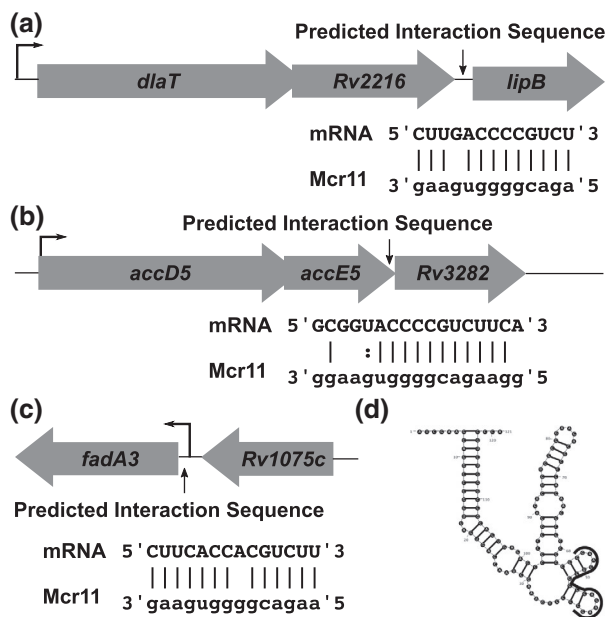
FIGURE 6 Bioinformatic modeling of Mcr11 targets reveals potential regulatory targets that are involved in central metabolism and cell division. (a) The organization of the *dlaT-lipB* locus, with the position and potential base-pairing interactions between the mRNA and Mcr11 is shown below. The transcriptional start site of the operon is shown with a thin black arrow. (b) As in (a), but for the *accD5-Rv3282* locus. Dashes indicate Watson–Crick base pairs, dots indicate non-Watson–Crick base pairs, and a blank space indicates no interaction between bases. (c) As in (a) and (b), but for the Rv1074c/*fadA3* locus. (d) The MFE secondary structure of Mcr11 as predicted by RNAStructure, with the portion of the sRNA predicted to interact with targets is shown in (a-c) outlined in black

upstream of Rv3282 are *accD5* and *accE5*, which are needed for a long chain aceyl-CoA carboxylase enzymatic complex that generates substrates for fatty acid and mycolic acid biosynthesis (Bazet Lyonnet et al., 2014, 2017). *fadA3* is expected to have a role in lipid degradation through beta-oxidation, although its role in the metabolic processes of Mtb has not been well defined.

Thus, we reasoned that media components, such as fatty acids, may impact the regulation of *fadA3* and the *dlaT*-Rv2216-*lipB* and/or *accD5*-*accE5*-Rv3282 operons. We used qRT-PCR to measure expression of predicted Mcr11-regulatory targets *fadA3*, *lipB* and Rv3282 in Wt versus *Δmcr11* strains. Gene expression was queried in stationary phase BCG and Mtb grown in media with (+OA) or without (−OA) added fatty acids to assess the impact of Mcr11 regulatory function in these conditions. Tween-80® is a hydrolysable detergent that releases a substantial amount of fatty acids (primarily oleic acid), and so was replaced with the non-hydrolysable detergent Tyloxapol in media lacking fatty acids. The *mcr11* complements included TSE4 with or without an intact copy of *abmR*. Levels of *phoP*, a response regulator expected to be independent of *mcr11* and *abmR*, and *pknA*, a serine-threonine protein kinase required for growth, were also measured.

Expression of Rv3282, Rv2216, *lipB* and *fadA3* was significantly de-repressed in Mtb*Δmcr11* compared to Wt Mtb in the absence, but not the presence, of fatty acids (Figure 7a,b). In contrast, levels

of *lipB* and *pknA* expression decreased in the *mcr11* Mtb mutant relative to Wt when fatty acids were present. Complementation of *mcr11* fully (Rv3282) or partially (Rv2216, *lipB*, *fadA3*) restored expression to Wt levels (Figure 7a). The expression of *accD5* (Rv3280) was significantly de-repressed and *accE5* (Rv3281) trended toward de-repression in Mtb*Δmcr11*, and complementation partially restored Wt expression levels of both genes (Supplemental Figure 6a). Expression of *dlaT* and *phoP* was not altered in Mtb (Figure 7a). From these data, we concluded that Mcr11-mediated regulation of Rv3282, Rv2216, *lipB* and *fadA3* expression in Mtb is affected by the levels of fatty acids in the media. In contrast, no Mcr11-dependent regulation of *lipB* was observed in BCG, although trend of higher Rv3282 expression in BCG*Δmcr11* relative to Wt BCG in the absence of fatty acids was observed (Figure 7c,d). These data demonstrate that *mcr11*-dependent regulation of specific target genes is responsive to the fatty acid content of the culture media, and suggest that Mcr11 has a role in regulating the central metabolism of Mtb.

2.7 | Mcr11 is required for optimal growth of BCG and Mtb without fatty acids

Optimal growth of Mtb on carbohydrate-based carbon sources requires appropriate *dlaT* expression (Shi & Ehrt, 2006; Venugopal et al., 2011), while *lipB*, *accD5* and *accE5* are essential for Mtb growth (Sassetti, Boyd, & Rubin, 2003; Sassetti & Rubin, 2003). Mutations in Rv3282 delay Mtb growth, even in nutrient rich media (Sassetti et al., 2003). Based on our observed regulation of these genes by Mcr11, we hypothesized that *Δmcr11* deleted strains would exhibit a growth defect when forced to utilize carbohydrate carbon sources for growth in media lacking a source of fatty acids.

BCG*Δmcr11* was severely growth-lagged and Mtb*Δmcr11* was moderately growth delayed compared to Wt bacteria when grown in media lacking added fatty acids (Figure 7e-h). In contrast, no growth differences were observed between Wt and *Δmcr11* mutant Mtb or BCG in media containing fatty acids. Complementation of mutant strains with *mcr11* partially complemented growth in BCG and fully restored growth to Wt levels in Mtb (Figure 7g,e). From these data, we conclude that *mcr11* has a role in the central metabolism and growth of BCG and Mtb.

2.8 | The bioinformatically predicted Mcr11 base-pairing sequence is required for the repression of lipB expression in Mtb

The necessity of the putative base-pairing interaction between Mcr11 and the *lipB* mRNA was tested by constructing a promoter:*GFPv* fusion reporter construct with or without disrupted potential base-pairing sequences in the *lipB* mRNA (Figure 8a) (Vasudeva-Rao & McDonough, 2008). The bases in the *lipB* promoter that were mutagenized were selected using TargetRNA to determine the minimal change required to disrupt the putative base-pairing interaction between the mRNA
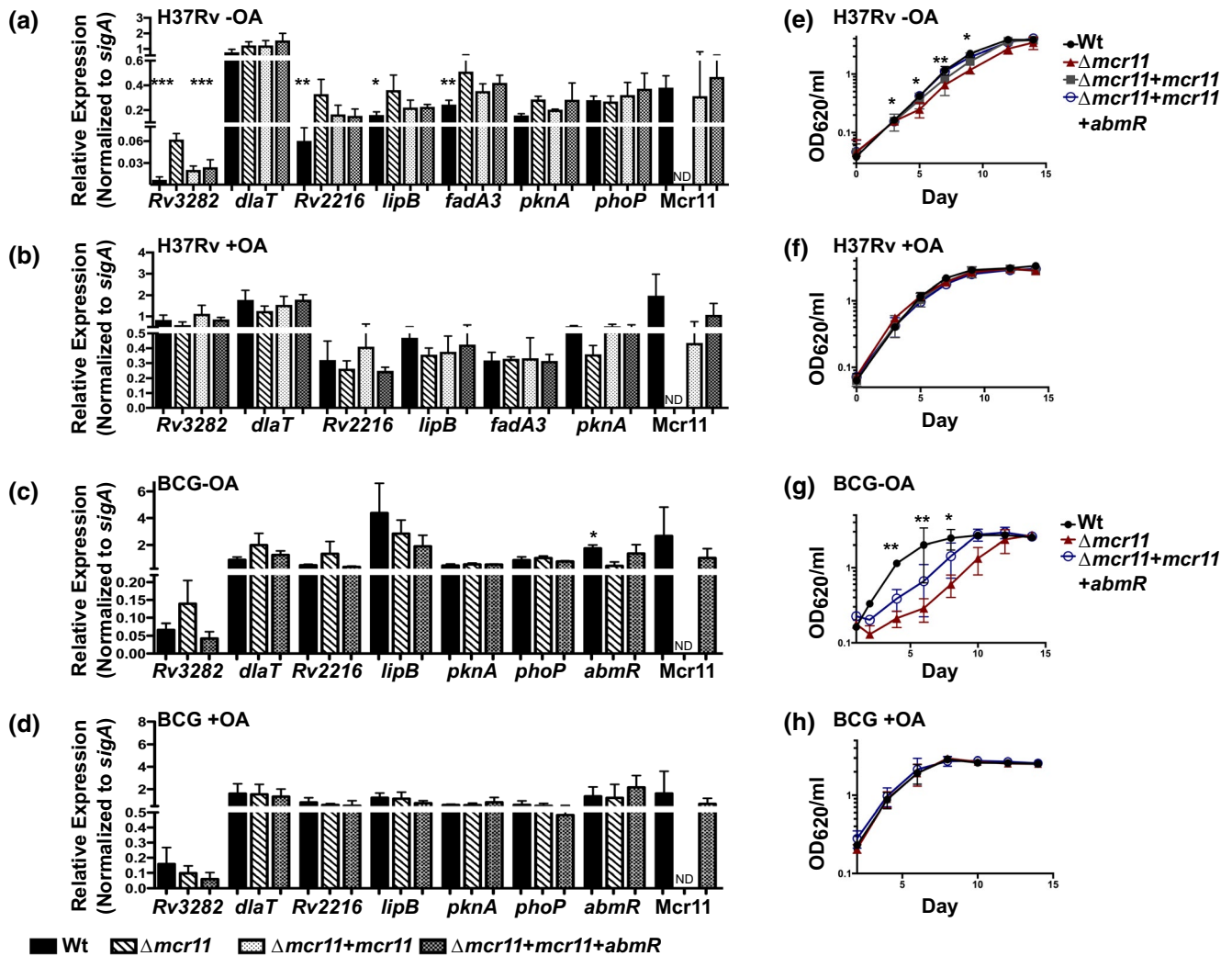
FIGURE 7 *Δmcr11* strains of BCG and Mtb are defective for growth in fatty-acid depleted media and predicted regulatory targets of Mcr11 are dysregulated at the mRNA level. (a) Mtb was grown for 12 days in under hypoxic (1.3% O_2, 5% CO_2), shaking conditions in −OA media (7H9 + 0.2% glycerol, 10% ADC and 0.05% Tween-80). Gene expression was measured by qRT-PCR and normalized to the reference gene *sigA*. Comparison made of each strain versus *Δmcr11*. Complementation strains included a single-copy of *mcr11* with TSE3 fused to *GFPv* or a single-copy of the *abmR* locus and *mcr11* with TSE4. (b) Mtb was grown for 7 days in under hypoxic, shaking conditions in + OA media (7H9 + 0.2% glycerol, 10% OADC and 0.05% Tween-80). Gene expression was measured by qRT-PCR and normalized to the reference gene *sigA*. (c) BCG was grown for 12 days in under hypoxic, shaking conditions in -OA media. Gene expression was measured by qRT-PCR and normalized to the reference gene *sigA*. (d) BCG was grown for 12 days in under hypoxic, shaking conditions in + OA media. Gene expression was measured by qRT-PCR and normalized to the reference gene *sigA*. (e) Growth curve of Mtb grown in hypoxic, shaking conditions in −OA media. Growth was surveyed by measuring the optical density at 620 nm (OD_{620}). (f) Growth curve of Mtb grown in hypoxic, shaking conditions in + OA media. Growth was surveyed by measuring OD_{620}. (g) As in (E), but with BCG. H. As in (F), but with BCG. Results are the means of three biological replicates. Statistical comparisons made of each strain versus *Δmcr11* using a one-way ANOVA with Bonferroni correction for multiple comparisons. Asterisks indicate significance as follows: *$p < .05$, **$p < .01$, ***$p < .001$, ****$p < .0001$ [Colour figure can be viewed at wileyonlinelibrary.com]

and Mcr11. Mtb was grown for 14 days in hypoxic, shaking conditions in media lacking fatty acids and expression from the Wt and mutagenized *lipB* internal promoters was measured using a GFPv fluorescence assay across growth phase. The Wt and mutant *lipB* promoters showed similar expression in early log phase, but the mutant promoter was significantly de-repressed at later time points (Figure 8b). The trend of de-repression observed in the mutagenized *lipB* promoter was similar to the de-repression of *lipB* expression that occurred in Mtb*Δmcr11* grown in the same condition (Figure 7a). These data demonstrate that the bioinformatically predicted Mcr11 base-pairing sequences are

required for the repression of *lipB* expression in Mtb by Mcr11, and they provide evidence for an mRNA-Mcr11 base-pairing mechanism of Mcr11-mediated repression of *lipB* expression in Mtb.

3 | DISCUSSION

This work identifies genes associated with central metabolism in Mtb as regulatory targets of the sRNA Mcr11. We also demonstrated that transcriptional termination and stable production

(a)

(b)
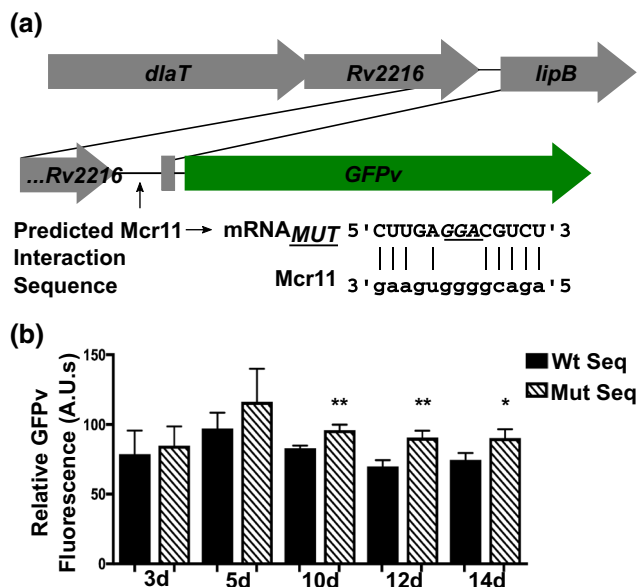
FIGURE 8 The bioinformatically predicted Mcr11 base-pairing sequence is required for the repression of *lipB* expression in Mtb. (a) The organization of the *dlaT-lipB* locus, with the internal promoter:*GFPv* fusion reporter construct and the disrupted potential base-pairing interactions between the *lipB* mRNA and Mcr11 is shown below. The bases in the *lipB* promoter that were mutagenized are indicated in underlined italics. (b) Mtb was grown for 14 days in under hypoxic (1.3% O_2, 5% CO_2), shaking conditions in −OA media (7H9 + 0.2% glycerol, 10% ADC and 0.05% Tyloxapol). Expression from the lipB internal promoter was measured using a GFPv fluorescence assay used to measure promoter activity at the indicated time points. Fluorescence is normalized to the OD_{620} of each sample. Expression from the *lipB* promoter with wild-type sequence is shown in black bars and expression from the mutagenized promoter is shown in slashed bars. Results are the means of three biological replicates. Statistical analysis conducted with a two-tailed Student's *T*-test to compare the expression of the *lipB* promoter with wild-type sequence to the mutagenized promoter at each time point. Asterisks indicate significance as follows: *$p < .05$, **$p < .01$, ***$p < .001$, ****$p < .0001$ [Colour figure can be viewed at wileyonlinelibrary.com]

of Mcr11 are enhanced by extended native sequence 3′ to *mcr11* along with the product of the divergently transcribed adjacent gene, *abmR* (Figure 9). The regulation of central metabolism in Mtb is consistent with *mcr11* expression profiles in response to growth phase and in vivo infection (Girardin et al., 2018; Pelly et al., 2012). However, the additional requirements for TB complex specific factors for stable Mcr11 expression were unexpected, and may have broader implications for understanding sRNA expression in Mtb.

3.1 | Mechanism of mcr11 transcriptional termination

Characterization of the factors required for efficient termination and stable expression of Mcr11 was a prerequisite for the complementation studies that confirmed Mcr11 regulatory targets. Protein coding mRNAs often can tolerate variable amounts of 5′ and 3′ flanking

sequence because the signals for protein expression are provided immediately upstream and within the open reading frame (ORF). In contrast, expression of functional sRNAs may be more dependent on RNA chaperones and/or processing factors, as well as cis-acting sequence elements at their transcriptional boundaries that are difficult to define at (Chae et al., 2011; Moores et al., 2017; Morita et al., 2015; Kriner, Sevostyanova, & Groisman, 2016; Shiflett et al., 2003). Although RNA chaperones have yet to be identified in mycobacteria, the roles of extended native 3′ sequences for expression of mycobacterial sRNAs warrant further investigation to determine whether *mcr11* is exceptional or representative of a larger group of sRNAs with regards to expression and stability requirements (Ishikawa, Otaka, Maki, Morita, & Aiba, 2012; Johnson et al., 2014; Moores et al., 2017; Regnier & Hajnsdorf, 2013; Sauer & Weichenrieder, 2011; Shiflett et al., 2003; Olejniczak & Storz, 2017).

A recent study of Rho function in Mtb (Botella, Vaubourgeix, Livny, & Schnappinger, 2017) found that depletion of Rho did not impact transcriptional boundaries at predicted RITs (Gardner et al., 2011; Mitra et al., 2008), demonstrating a clear separation in the populations of transcripts terminated by RITs and Rho-dependent mechanisms. While we found that TSEs promote expression of Mcr11, their underlying mechanism remains unclear and our data do not precisely fit either the current RIT or Rho-dependent termination models (Table 1). We propose a model in which *mcr11* processing occurs immediately following, or concurrent with, Rho-dependent termination.

Rho-independent termination is considered 'intrinsic' because extrinsic accessory factors are not required for function (Ray-Soni et al., 2016). Our results clearly indicate that production of stable Mcr11 requires factors other than the TSEs (Figures 2d and 4). The species-specific effects we observed for *mcr11* termination measured by the GFPv reporter assays suggest that bacterial-specific factors affect the efficiency of *mcr11* termination itself, although the effects on Mcr11 stability are more striking (Figures 2–4).

Rho utilization (rut) sites are degenerate and difficult to predict using bioinformatics approaches, but transcripts terminated by Rho tend to have C-enriched, G-depleted 3′ ends that are thought to be unstructured (Peters et al., 2009). It is not clear if there is a rut site within *mcr11*, as the sequences downstream of the 3′ end of Mcr11 are predicted to be highly structured and are rich in both G and C (Figure 1). A run of 6Cs (nucleotides 93–98) occurs within Mcr11, but this region may be highly structured (Figure 1). In contrast, Mcr11 TSEs 2–4, which contributed strongly to the termination of Mcr11, all possess C-rich loops in their predicted secondary structures that could be rut sites (Figure 1). Rho-significant regions (RSRs) reported in the Botella et al study (Botella et al., 2017) include an RSR that begins 6 nt downstream of the mapped 3′ end of Mcr11, that is characterized as a region of general antisense transcription. The presence of this RSR is consistent with the possibility that *mcr11* expression is Rho-terminated. Mcr10 (*ncRv1157a*) is also proximal to an RSR (Botella et al., 2017). Future work is needed to address the importance of Rho-dependent termination for mycobacterial sRNAs.

In *Escherichia coli*, multiple trans-acting factors are known to modulate termination and anti-termination of Rho-terminated sRNAs

**TABLE 1** Comparison of transcription termination types

Features	Rho-Dependent	Intrinsic	Mcr11
Predicted hairpin in 3' sequence		✓	✓
Unstructured, C-rich 3' sequence	✓		
Poly U-tract in 3' sequence		✓	
Extrinsic factor(s) required	✓		✓
Transcription factor may impact functionality	✓	✓	✓

(Rabhi et al., 2011). AbmR, an ATP-responsive DNA-binding transcription factor that activates *mcr11* expression (Girardin et al., 2018), was found here to also positively regulate termination efficiency of *mcr11* (Supplemental Figure 3). Despite the high similarity between *abmR* and its Msm orthologue (Girardin et al., 2018), *MSM_5010* failed to strongly activate *mcr11* expression and Mcr11 transcripts were unstable in Msm, even though provision of *abmR* in trans enhanced Mcr11 levels. It is possible that AbmR interacts directly with RNAP or Rho to affect termination, or recruits an as yet undefined trans-acting factor that modulates Mcr11 termination in Mtb. For example, Rv1222 is a mycobacterial DNA-binding protein that was found to slow the rate of RNA synthesis through direct interaction with RNAP, and AbmR may function in a similar manner to promote termination at the *mcr11* locus (Rudra, Prajapati, Banerjee, Sengupta, & Mukhopadhyay, 2015).

The discrete 3′ end of mature Mcr11 observed by Northern blot is consistent with a processed or precisely terminated RNA, as transcription through TSEs would otherwise result in significantly longer RNA products. Processing of the 3′ ends of mycobacterial sRNAs has been proposed (Tsai et al., 2013), and a recent report identified a hypoxia-regulated mycobacterial sRNA that is extensively processed at its 3′ end (Moores et al., 2017). The observed size variants of specific sRNA species in response to host-associated stress conditions (Arnvig & Young, 2009) provide further evidence for processing of sRNAs in mycobacteria. Recent work has demonstrated that Rho terminated transcripts have processed 3′ ends immediately downstream of a stable stem-loop (Dar & Sorek, 2018). While few RNA processing enzymes of mycobacteria have been well characterized, the Mtb genome encodes many known RNases with varying sequence specificities (Abendroth et al., 2014; Taverniti, Forti, Ghisotti, & Putzer, 2011; Uson, Ordonez, & Shuman, 2015; Zeller et al., 2007; Zhu et al., 2008, 2006). We speculate that unidentified TB-complex RNA chaperones and/or modifying enzymes contribute to Mcr11 stability, and that their absence in Msm results in Mcr11 degradation.

3.2 | Regulation of predicted targets of Mcr11

Oleic acid is the main fatty acid present in rich mycobacterial media formulations, provided either directly as oleic acid or in the hydrolyzable, non-ionic detergent Tween-80®. The
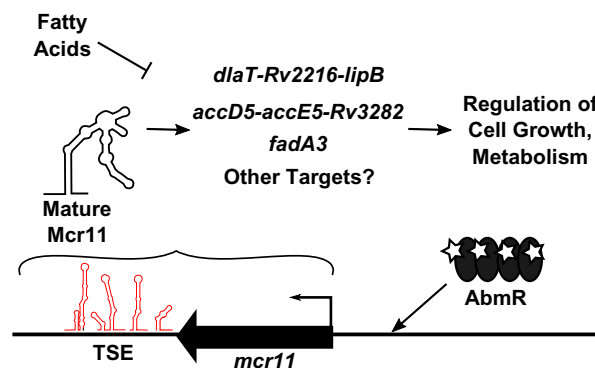
FIGURE 9 Model of Mcr11 function in Mtb. Expression of *mcr11* is activated by advancing growth phase and the ATP-binding transcription factor AbmR. Native 3′ sequence elements (TSEs, predicted secondary structures shown in red) promote the transcriptional termination of Mcr11 (shown in black). Mcr11 regulates the expression of genes involved in the central metabolism and growth of Mtb through base-pairing interaction between Mcr11 and target mRNAs. This regulation and the importance of Mcr11 for °ptimal growth of Mtb is affected by the presence of fatty acids [Colour figure can be viewed at wileyonlinelibrary.com]

presence of Tween-80® can alter acid resistance (Vandal, Pierini, Schnappinger, Nathan, & Ehrt, 2008), enhances the growth of mycobacteria when combined with glucose or glycerol (Lofthouse et al., 2013; Schaefer & Lewis, 1965) and increases the uptake of glucose by BCG (Lofthouse et al., 2013; Schaefer & Lewis, 1965). While we observed no increase in sensitivity to acid in BCGΔ*mcr11* or BCGΔ*abmR* (data not shown), *mcr11* was required for growth on media lacking added fatty acids. Nutrient rich media is often used in batch culture experimentation with Mtb, and the potential confounding effect of multiple nutrient sources on characterizing the essentiality and function of gene products has recently gained appreciation (DeJesus et al., 2017; Griffin et al., 2011). Future studies characterizing nutrient uptake in Mtb and BCG strains of Δ*mcr11* or Δ*abmR* will further our understanding of the nutrient-related growth defects of these strains.

Dihydrolipoamide acyltransferase (DlaT) and BkdC, a component of the Lpd-dependent branched chain keto-acid dehydrogenase (BCKADH), are critical for Mtb pathogenesis and known to be lipoylated in Mtb (Venugopal et al., 2011). Lipoylation in Mtb is presumed to depend solely on lipoate synthesis by the enzymes LipA and the Mcr11 target LipB, as scavenging and import pathways are apparently lacking (Spalding & Prigge, 2010). Rv3282 has homology to Maf, a septum inhibition protein conserved across all domains of life (Hamoen, 2011; Tchigvintsev et al., 2013). Despite *mcr11*-dependent regulation of *Rv3282* in the absence of fatty acids, MtbΔ*mcr11* did not have a filamentous cell morphology (data not shown) and the function of Rv3282 in Mtb has not been defined. The regulation of Mcr11's targets was responsive to the fatty acid content of the growth media, and it will be important to determine if the observed growth defects of MtbΔ*mcr11* are due to the dysregulation of *fadA3*, *lipB* and Rv3282, or if there are additional targets of Mcr11 regulation that account for this phenotype (Figure 9). Additionally, the

role of Mcr11 in supporting the growth and persistence of Mtb in response to nutrient availability and growth arrest should be explored.

Mcr11-dependent regulation of *lipB*, *fadA3* and Rv3282 expression was expected to occur through base-paring with the mRNA, and we demonstrated that the predicted base-pairing sequences were required for repression of *lipB* expression (Figure 8). The sRNA RyhB is known to differentially regulate expression of individual genes within the *iscRSUA* operon, resulting in down-regulation of the *icsSUA* genes while maintaining expression of *iscR* (Desnoyers, Morissette, Prevost, & Masse, 2009). This mechanism requires an intra-cistronic base-pairing dependent translational blockade of *iscS*, followed by recruitment of RNaseE and selective degradation of the 3′ end of the mRNA. The position of two putative Mcr11 base-pairing sites within target gene operons raises multiple possibilities for *mcr11*-mediated regulation of co-transcribed genes that will be an intriguing topic for future study. We noted that the *mcr11* target interaction site within the intergenic region of Rv2216 and *lipB* had identical spacing to that of Rv1075c and *fadA3*, although the significance of this architecture is unknown.

This study shows that the transcriptional termination and stability of the sRNA Mcr11 are enhanced by extended, native 3′ sequence elements (TSEs) in TB complex mycobacteria. The role of AbmR in *mcr11* expression was extended from that of a transcriptional activator to include enhancement of *mcr11* transcriptional termination. Our observation that bacterial species-specific factors govern sRNA stability in mycobacteria may also extend to other sRNAs. Combined use of bioinformatic and molecular tools established fatty acid responsive, *mcr11*-dependent gene regulation in Mtb and provides a versatile strategy for the continued search of sRNA function in pathogenic mycobacteria. Future work defining the precise roles of the sRNA Mcr11 in regulating the growth and metabolism of Mtb will greatly advance our understanding of this important pathogen.

4 | EXPERIMENTAL PROCEDURES

4.1 | Bacterial strains and growth conditions

Mycobacterium tuberculosis H37Rv (Mtb) (ATCC 25618) and *Mycobacterium bovis* BCG (BCG) (Pasteur strain, Trudeau Institute) were grown on 7H10 agar (Difco) supplemented with 10% oleic acid-albumin-dextrose-catalase (OADC) (Becton Dickson and Company) and 0.01% cycloheximide or in Middlebrook 7H9 liquid medium (Difco) supplemented with 10% (vol/vol) OADC, 0.2% (vol/vol) glycerol and 0.05% (vol/vol) Tween-80 (Sigma-Aldrich) in physiologically relevant shaking, hypoxic conditions (1.3% O_2, 5% CO_2) (Florczyk, McCue, Stack, Hauer, & McDonough, 2001) for promoter::reporter fusion assays and Northern blot analysis. *Mycobacterium smegmatis* mc^{2}155 (Msm) (ATCC 700,048) was grown in Middlebrook 7H9 liquid medium (Difco) supplemented with 10% (vol/vol) OADC, 0.2% (vol/vol) glycerol and 0.05% (vol/vol) Tween-80 (Sigma-Aldrich), shaking in ambient air for promoter::reporter fusion assays and Northern blot analysis. All

experiments were started from low-passage frozen stocks. For cloning experiments, *Escherichia coli* strains were grown on Luria-Bertani (Difco) agar plates or in liquid broth. Growth media and plates were supplemented with 50 μg/mL of hygromycin, 25 μg/mL of kanamycin (Sigma-Aldrich) for selection of clones. All bacterial cultures were incubated at 37°C.

4.2 | Mutant strain construction

Knockout strains of *mcr11* in Mtb and BCG genetic backgrounds were generated using homologous recombination (Bardarov et al., 2002) to replace nucleotides 1–100 with a hygromycin resistance cassette. Disruption of *mcr11* was confirmed with polymerase chain reaction (PCR) (Supplemental Figure 1b,c) and Northern blot analysis (Supplemental Figure 1d,e.). Several complementation constructs were created to restore Mcr11 expression. Sequence from the corrected *abmR* (*Rv1265*) start site (Gazdik et al., 2009) to the end of the *Rv1264* ORF was amplified by PCR and cloned downstream of the *efTu* (Rv0685) promoter in the multi-copy plasmid pMBC280, creating pMBC1211. PCR was used to amplify varying lengths of sequence from the end of the *Rv1264* ORF through the end of the *abmR* ORF, and they were cloned it into pMBC409, which contains a kanamycin resistance marker, to create pMBC2040, pMBC2041 and pMBC2042 (Supplemental Figure 1a). Complementation plasmids were sequenced to verify that the desired sequences had been correctly incorporated and then used to transform Mtb and BCG by electroporation. A complete list of plasmids used in this study is shown in Supplemental Table 1 and primers are shown in Supplemental Table 2.

4.3 | Mapping the 3′ end of Mcr11

RNA was harvested from late-log phase Mtb and the 3′ end of Mcr11 was mapped using the miScript Reverse Transcription Kit (Qiagen) (Beauregard et al., 2013) and a gene-specific primer. The reaction product was cloned into pCRII-TOPO vector (Life Technologies) and 10 positive clones were subjected to Sanger sequencing. The sequences were mapped back to the chromosome of Mtb.

4.4 | Bioinformatic modeling of Mcr11

Secondary structure modeling of Mcr11 and putative native intrinsic terminators was performed using RNAstructure using default parameters (Mathews, 2006). A synthetic terminator (tt$_{sbi}$B) (Huff, Czyz, Landick, & Niederweis, 2010) was modeled onto Mcr11 as well. Secondary structure modeling of Mcr11 was performed using RNAstructure (Mathews, 2006). Using the previously published 5′ and 3′ boundaries of Mcr11, minimum free energy (MFE) and centroid structures for Mcr11 derived from CentroidFold (using the CONTRAfold inference engine), Mfold, NUPACK, RNAfold and RNAStructure algorithms were created (Ding, Chan, & Lawrence, 2004; Mathews, 2006; Sato, Hamada, Asai, &

Mituyama, 2009; Zadeh et al., 2011; Zuker, 2003). Base-pair drawings of predicted RNA secondary structures were either directly exported from the software used, or created with Visualization Applet for RNA (VARNA) (Darty, Denise, & Ponty, 2009) and simplified line drawings were made in Inkscape (inkscape.org).

Regulatory targets of Mcr11 in Mtb were predicted using TargetRNA (Tjaden, 2008) and TargetRNA2 algorithms (Kery et al., 2014), set to default parameters (Table3). Where possible, the position of predicted regions of base-paring between Mcr11 and a putative regulatory target was evaluated against known 5′ ends of mRNAs in Mtb (Cortes et al., 2013) (Table 3).

4.5 | Promoter:reporter fusion assays

Promoter:*lacZ* fusions were created to compare the relative transcriptional activities from DNA sequences spanning the intergenic space between *Rv1264* and *abmR*, and *mcr11* and *abmR* (Supplemental Figure 2). The promoters of *gyrB* (*Rv0005*) and *tuf* (*Rv0685*) were used as positive controls, and a promoterless construct was used as a negative control. The relevant constructs were transformed into wild-type (Wt) strains of BCG and Mtb and assayed for β-galactosidase activity in late-log phase cultures grown in ambient, shaking conditions by adding 5-acetylaminofluoresceindi-β-D-galactopyranoside (C₂FDG; Molecular Probes) and measuring fluorescence in a Cytofluor 4000 fluorometer (PerSeptive Biosystems) as described previously (Vasudeva-Rao & McDonough, 2008).

Constructs including the *mcr11* promoter, Mcr11 sequence and various potential intrinsic terminator sequences were fused to the reporter green fluorescent protein Venus (*GFPv*) on an integrating plasmid as previously described (Girardin et al., 2018). A GFPv fluorescence assay was used to measure promoter activity and read-through of the putative intrinsic terminators of Mcr11 in Msm, BCG and Mtb.

At mid-log phase and late stationary phase, aliquots of recombinant strains were collected and gently sonicated (setting 4, 4 pulses of 5″ on time interspersed by 5′ off time) using a Virsonic 475 Ultrasonic Cell Disrupter with a cup horn attachment (VirTis Company) before duplicate samples were diluted 1:1 in fresh media. The level of fluorescence in arbitrary units from the GFPv reporter strain was detected using the CytoFluor Multi-Well Plate Reader Series 4,000 (PerSeptive Biosystems) at 485 nm excitation and 530 nm emission. The optical density (OD) at 620 nm was read using a Tecan Sunrise® microplate reader and fluorescence levels were normalized to 10^6 bacteria. A promotorless (-) construct was used as a negative control and the promoters P*tuf* and P*gyr* served as positive controls. The % termination was calculated by dividing the observed GFPv fluorescence in arbitrary units of each indicated terminator construct by the amount of GFPv fluorescence in arbitrary units measured from the *mcr11* promoter.

Late stationary phase reporter strains of BCG and Mtb were diluted with fresh media to an OD620 nm of 1.25 in a 12-well plate, and then subjected to a variety of cellular stressors for a 24 hr period in shaking, hypoxic conditions (1.3% O_2, 5% CO_2). Cells were treated with 250 μM diethyltriamine-NO (DETA-NO)

(Sigma-Aldrich), 1 μg per mL of ofloxacin (OFX), 0.28 μg per mL of rifampacin (RIF), 53 μg per ml of bedaquiline (BDQ), or 0.1% dimethyl sulfoxide (DMSO) vehicle control. GFPv fluorescence in arbitrary units per 106 bacteria (by measured OD at 620 nm) was monitored as described above, and percent termination was calculated relative to P*mcr11* controls.

4.6 | Fluorescence-activated cell sorting analysis

Fluorescence-activated cell sorting analysis was performed on Msm samples that had been fixed with 4% paraformaldehyde (PFA) in phosphate-buffered saline (PBS) at pH 7.0 for 30 min at room temperature. Fixation was quenched pH-adjusted glycine, and cells were washed three times with PBS. Cells were diluted approximately 1:500 in DPBS and subjected to FACS analysis with a FACS Calibur (Becton Dickson) as previously described (Purkayastha, McCue, & McDonough, 2002). Data were collected for 20,000 events per sample and analyzed in CellQuest software (Becton Dickenson).

4.7 | RNA isolation

Total RNA was harvested from Msm, BCG and Mtb after cultures were treated 0.5 M final GTC solution (5.0 M guanadinium isothiocyanate, 25 mM sodium citrate, 0.5% sarkosyl, and 0.1 M 2-β-mercaptoethanol) and pelleted at 4°C. Pelleted cells were resuspended in TRIzol Reagent (Invitrogen) and cells were disrupted with 0.1 mm zirconia-silica beads (BioSpec Products) and three 70-s high-speed pulse treatments in a bead-beater (BioSpec Products). RNA was recovered from lysates with Direct-zol Mini Prep columns (Zymo) per the manufacturer's protocol. RNA was eluted from the column with nuclease free-water, treated with DNaseI (Qiagen) for 20 min at room temperature, and isopropanol precipitated. One μg of total RNA was screened for DNA contamination by PCR using primers KM1309 and KM1310 internal to the sigA ORF. The quality of each RNA sample was assessed by running 1.0 μg of DNA-free RNA on a 0.1% (weight/vol) SDS-agarose gel and visualizing intact 23S, 16S, and 5S ribosomal RNA bands after staining with ethidium bromide (Sigma-Aldrich).

4.8 | Northern blots

High quality DNA-free total RNA isolated from Msm, BCG and Mtb was used for Northern blot analysis of Mcr11 expression. About 3–10 μg RNA was separated on a 10% 8 M urea PAGE run at a constant current of 20 mA for 1–1.5 hr. The gel was electroblotted onto a Hybond N (Millipore) nylon membrane using a wet transfer system (Bio-Rad Laboratories) as previously described (Girardin, in prep). Blots were UV cross-linked and baked at 80°C for 2 hr prior to prehybridization at 42°C for 1 hr in Rabid-Hyb Buffer (GE Healthcare Life Sciences). Hybridization with α-^{32}P-ATP end-labeled DNA oligo

probes was performed at 42°C for 2–16 hr. Blots were washed per the manufacturer's protocol and exposed to phosphor-screens for visualization. Densitometry was completed using ImageQuant software.

4.9 | Generation of mycobacterial cell lysates and Western blotting

Strains of BCG and Mtb were grown in the desired condition, and pelleted and washed twice in ice-cold Dulbecco's phosphate-buffered saline, calcium and magnesium free (DPBS-CMF), with 0.2% protease inhibitor (Sigma-Aldrich). Cell pellets were resuspended in 1/25 volume lysis buffer (0.3% SDS, 200 mM DTT, 28 mM Tris-Hcl, 22 mM Tris-Base and 1% protease inhibitor cocktail) and disrupted by two rounds of high-powered sonication at 4°C with Virsonic 475 Ultrasonic Cell Disrupter with a cup horn attachment (VirTis Company) interspersed with 10 freeze-thaw cycles as previously described (Girardin et al., 2018). Lysate was cleared by centrifugation and the cleared lysate was heat-killed at 95°C before quantification with a NanoDrop 2000 (Thermo Scientific).

A total of 30 µg protein of each sample was separated by 12%–15% Tris-glycine SDS-PAGE, and gels were immunoblotted on Immobilon-P membranes (Millipore) for 1h at 1 mA/cm^2 using a wet transfer system (Bio-Rad Laboratories). Blots were blocked and proved with 1° antibody in 5% milk (vol/vol) in 50 mM Tris-buffered saline with 0.05% (vol/vol) Tween-20 (Fisher Scientific). Monoclonal antibodies against Mtb GlcB (Gene Rv1837c), Clone α-GlcB (produced in vitro NR-13799) was obtained through the NIH Biodefense and Emerging Infections Research Resources Repository, NIAID, NIH. Polyclonal mouse AbmR anti-serum was previously generated in-house (Girardin et al., 2018). Primary antibodies were detected with peroxidase conjugated goat secondary antibody and enhanced chemiluminescence (ECL) Western blotting detection reagent (Thermo Scientific).

4.10 | Growth curve analysis

The growth of BCG and Mtb in hypoxic (1.3% O2, 5% CO2), shaking conditions was monitored by measuring the optical density at 620 nm (OD620) of gently sonicated aliquots of cells with a Tecan Sunrise® microplate reader. Cultures were grown in vented T25 tissue culture flasks (Corning), and time points were in single or multi-day intervals. Growth comparisons between Middlebrook 7H9 + 0.2% glycerol, 10% OADC and 0.05% Tween-80 (+OA) or in Middlebrook 7H9 + 0.2% glycerol, 10% ADC and 0.05% Tyloxapol (−OA) were made.

DATA SHARING

The data that support the findings of this study are available in the supplementary material of this article.

CONFLICTS OF INTEREST

None declared.

ORCID

Kathleen A. McDonough (iD) https://orcid.org/0000-0002-2813-6263

REFERENCES

Abendroth, J., Ollodart, A., Andrews, E. S., Myler, P. J., Staker, B. L., Edwards, T. E., … Grundner, C. (2014). *Mycobacterium tuberculosis* Rv2179c protein establishes a new exoribonuclease family with broad phylogenetic distribution. *Journal of Biological Chemistry*, *289*, 2139–2147.

Arnvig, K. B., Comas, I., Thomson, N. R., Houghton, J., Boshoff, H. I., Croucher, N. J., … Young, D. B. (2011). Sequence-based analysis uncovers an abundance of non-coding RNA in the total transcriptome of *Mycobacterium tuberculosis*. *PLoS Path*, *7*, e1002342. https://doi.org/10.1371/journal.ppat.1002342

Arnvig, K. B., & Young, D. B. (2009). Identification of small RNAs in *Mycobacterium tuberculosis*. *Molecular Microbiology*, *73*, 397–408.

Bardarov, S., Bardarov, S., Jr., Pavelka, M. S., Jr., Sambandamurthy, V., Larsen, M., Tufariello, J., … Jacobs, W. R., Jr. (2002). Specialized transduction: An efficient method for generating marked and unmarked targeted gene disruptions in Mycobacterium tuberculosis, M. bovis BCG and M. smegmatis. *Microbiology*, *148*, 3007–3017. https://doi.org/10.1099/00221287-148-10-3007

Bazet Lyonnet, B., Diacovich, L., Cabruja, M., Bardou, F., Quemard, A., Gago, G., & Gramajo, H. (2014). Pleiotropic effect of AccD5 and AccE5 depletion in acyl-coenzyme A carboxylase activity and in lipid biosynthesis in mycobacteria. *PLoS ONE*, *9*, e99853. https://doi.org/10.1371/journal.pone.0099853

Bazet Lyonnet, B., Diacovich, L., Gago, G., Spina, L., Bardou, F., Lemassu, A., … Gramajo, H. (2017). Functional reconstitution of the *Mycobacterium tuberculosis* long-chain acyl-CoA carboxylase from multiple acyl-CoA subunits. *FEBS Journal*, *284*, 1110–1125.

Beauregard, A., Smith, E. A., Petrone, B. L., Singh, N., Karch, C., McDonough, K. A., & Wade, J. T. (2013). Identification and characterization of small RNAs in *Yersinia pestis*. *RNA Biology*, *10*, 397–405.

Bergkessel, M., Basta, D. W., & Newman, D. K. (2016). The physiology of growth arrest: Uniting molecular and environmental microbiology. *Nature Reviews Microbiology*, *14*, 549–562.

Betts, J. C., Lukey, P. T., Robb, L. C., McAdam, R. A., & Duncan, K. (2002). Evaluation of a nutrient starvation model of *Mycobacterium tuberculosis* persistence by gene and protein expression profiling. *Molecular Microbiology*, *43*, 717–731.

Botella, L., Vaubourgeix, J., Livny, J., & Schnappinger, D. (2017). Depleting Mycobacterium tuberculosis of the transcription termination factor Rho causes pervasive transcription and rapid death. *Nature Communications*, *8*, 14731. https://doi.org/10.1038/ncomms14731

Bryk, R., Gold, B., Venugopal, A., Singh, J., Samy, R., Pupek, K., … Nathan, C. (2008). Selective killing of nonreplicating mycobacteria. *Cell Host & Microbe*, *3*, 137–145. https://doi.org/10.1016/j.chom.2008.02.003

Chae, H., Han, K., Kim, K. S., Park, H., Lee, J., & Lee, Y. (2011). Rho-dependent termination of *ssrS* (6S RNA) transcription in *Escherichia coli*: Implication for 3′ processing of 6S RNA and expression of downstream *ygfA* (putative 5-formyl-tetrahydrofolate cyclo-ligase). *Journal of Biological Chemistry*, *286*, 114–122.

Cortes, T., Schubert, O. T., Rose, G., Arnvig, K. B., Comas, I., Aebersold, R., & Young, D. B. (2013). Genome-wide mapping of transcriptional start sites defines an extensive leaderless transcriptome in *Mycobacterium tuberculosis*. *Cell Reports*, *5*, 1121–1131. https://doi.org/10.1016/j.celrep.2013.10.031

Czyz, A., Mooney, R. A., Iaconi, A., & Landick, R. (2014). Mycobacterial RNA polymerase requires a U-tract at intrinsic terminators and is aided by NusG at suboptimal terminators. *Mbio*, *5*, e00931. https://doi.org/10.1128/mBio.00931-14

Dar, D., & Sorek, R. (2018). High-resolution RNA 3′ends mapping of bacterial Rho-dependent transcripts. *Nucleic Acids Research*, *46*, 6797–6805. https://doi.org/10.1093/nar/gky274

Darty, K., Denise, A., & Ponty, Y. (2009). VARNA: Interactive drawing and editing of the RNA secondary structure. *Bioinformatics*, *25*, 1974–1975. https://doi.org/10.1093/bioinformatics/btp250

DeJesus, M. A., Gerrick, E. R., Xu, W., Park, S. W., Long, J. E., Boutte, C. C., … Ioerger, T. R. (2017). Comprehensive essentiality analysis of the *Mycobacterium tuberculosis* genome via saturating transposon m*utagenesis*, *MBio*, *8*(1), e02133–16. https://doi.org/10.1128/mBio.02133-16

Desnoyers, G., Morissette, A., Prevost, K., & Masse, E. (2009). Small RNA-induced differential degradation of the polycistronic mRNA iscRSUA. *EMBO Journal*, *28*, 1551–1561. https://doi.org/10.1038/emboj.2009.116

DiChiara, J. M., Contreras-Martinez, L. M., Livny, J., Smith, D., McDonough, K. A., & Belfort, M. (2010). Multiple small RNAs identified in *Mycobacterium bovis* BCG are also expressed in *Mycobacterium tuberculosis* and *Mycobacterium smegmatis*. *Nucleic Acids Research*, *38*, 4067–4078. https://doi.org/10.1093/nar/gkq101

Ding, Y., Chan, C. Y., & Lawrence, C. E. (2004). Sfold web server for statistical folding and rational design of nucleic acids. *Nucleic Acids Research*, *32*, W135–141. https://doi.org/10.1093/nar/gkh449

Dubey, A. K., Baker, C. S., Romeo, T., & Babitzke, P. (2005). RNA sequence and secondary structure participate in high-affinity CsrA-RNA interaction. *RNA*, *11*, 1579–1587. https://doi.org/10.1261/rna.2990205

Florczyk, M. A., McCue, L. A., Stack, R. F., Hauer, C. R., & McDonough, K. A. (2001). Identification and characterization of mycobacterial proteins differentially expressed under standing and shaking culture conditions, including Rv2623 from a novel class of putative ATP-binding proteins. *Infection and Immunity*, *69*, 5777–5785. https://doi.org/10.1128/IAI.69.9.5777-5785.2001

Gardner, P. P., Barquist, L., Bateman, A., Nawrocki, E. P., & Weinberg, Z. (2011). RNIE: Genome-wide prediction of bacterial intrinsic terminators. *Nucleic Acids Research*, *39*, 5845–5852. https://doi.org/10.1093/nar/gkr168

Garton, N. J., Waddell, S. J., Sherratt, A. L., Lee, S. M., Smith, R. J., Senner, C., … Barer, M. R. (2008). Cytological and transcript analyses reveal fat and lazy persister-like bacilli in tuberculous sputum. *PLoS Medicine*, *5*, e75. https://doi.org/10.1371/journal.pmed.0050075

Gazdik, M. A., Bai, G., Wu, Y., & McDonough, K. A. (2009). Rv1675c (cmr) regulates intramacrophage and cyclic AMP-induced gene expression in *Mycobacterium tuberculosis*-complex mycobacteria. *Molecular Microbiology*, *71*, 434–448.

Gerrick, E. R., Barbier, T., Chase, M. R., Xu, R., Francois, J., Lin, V. H., … Fortune, S. M. (2018). Small RNA profiling in *Mycobacterium tuberculosis* identifies MrsI as necessary for an anticipatory iron sparing response. *Proceedings of the National Academy of Sciences of the United States of America*, *115*, 6464–6469.

Girardin, R. C., Bai, G., He, J., Sui, H., & McDonough, K. A. (2018). AbmR (Rv1265) is a Novel transcription factor of *Mycobacterium tuberculosis* that regulates host cell association and expression of the non-coding small RNA Mcr11. *Molecular Microbiology*, *110*(5), 811–830. https://doi.org/10.1111/mmi.14126

Gomez, J. E., & McKinney, J. D. (2004). *M. tuberculosis* persistence, latency, and drug tolerance. *Tuberculosis (Edinb)*, *84*, 29–44. https://doi.org/10.1016/j.tube.2003.08.003

Griffin, J. E., Gawronski, J. D., Dejesus, M. A., Ioerger, T. R., Akerley, B. J., & Sassetti, C. M. (2011). High-resolution phenotypic profiling defines genes essential for mycobacterial growth and cholesterol catabolism. *PLoS Path*, *7*, e1002251. https://doi.org/10.1371/journal.ppat.1002251

Hamoen, L. W. (2011). Cell division blockage: But this time by a surprisingly conserved protein. *Molecular Microbiology*, *81*, 1–3. https://doi.org/10.1111/j.1365-2958.2011.07693.x

Hnilicova, J., Jirat Matejckova, J., Sikova, M., Pospisil, J., Halada, P., Panek, J., & Krasny, L. (2014). Ms1, a novel sRNA interacting with the RNA polymerase core in mycobacteria. *Nucleic Acids Research*, *42*, 11763–11776. https://doi.org/10.1093/nar/gku793

Honaker, R. W., Dhiman, R. K., Narayanasamy, P., Crick, D. C., & Voskuil, M. I. (2010). DosS responds to a reduced electron transport system to induce the *Mycobacterium tuberculosis* DosR regulon. *Journal of Bacteriology*, *192*, 6447–6455. https://doi.org/10.1128/JB.00978-10

Huff, J., Czyz, A., Landick, R., & Niederweis, M. (2010). Taking phage integration to the next level as a genetic tool for mycobacteria. *Gene*, *468*, 8–19. https://doi.org/10.1016/j.gene.2010.07.012

Ignatov, D. V., Salina, E. G., Fursov, M. V., Skvortsov, T. A., Azhikina, T. L., & Kaprelyants, A. S. (2015). Dormant non-culturable *Mycobacterium tuberculosis* retains stable low-abundant mRNA. *BMC Genomics*, *16*, 954. https://doi.org/10.1186/s12864-015-2197-6

Iona, E., Pardini, M., Mustazzolu, A., Piccaro, G., Nisini, R., Fattorini, L., & Giannoni, F. (2016). *Mycobacterium tuberculosis* gene expression at different stages of hypoxia-induced dormancy and upon resuscitation. *Journal of Microbiology (Seoul, Korea)*, *54*, 565–572. https://doi.org/10.1007/s12275-016-6150-4

Ishikawa, H., Otaka, H., Maki, K., Morita, T., & Aiba, H. (2012). The functional Hfq-binding module of bacterial sRNAs consists of a double or single hairpin preceded by a U-rich sequence and followed by a 3′ poly(U) tail. *RNA*, *18*, 1062–1074. https://doi.org/10.1261/rna.031575.111

Johnson, C. M., Chen, Y., Lee, H., Ke, A., Weaver, K. E., & Dunny, G. M. (2014). Identification of a conserved branched RNA structure that functions as a factor-independent terminator. *Proceedings of the National Academy of Sciences of the United States of America*, *111*, 3573–3578. https://doi.org/10.1073/pnas.1315374111

Kery, M. B., Feldman, M., Livny, J., & Tjaden, B. (2014). TargetRNA2: Identifying targets of small regulatory RNAs in bacteria. *Nucleic Acids Research*, *42*, W124–129. https://doi.org/10.1093/nar/gku317

Kriner, M. A., Sevostyanova, A., & Groisman, E. A. (2016). Learning from the leaders: Gene regulation by the transcription termination factor Rho. *Trends in Biochemical Sciences*, *41*, 690–699. https://doi.org/10.1016/j.tibs.2016.05.012

Lofthouse, E. K., Wheeler, P. R., Beste, D. J., Khatri, B. L., Wu, H., Mendum, T. A., … McFadden, J. (2013). Systems-based approaches to probing metabolic variation within the *Mycobacterium tuberculosis* complex. *PLoS ONE*, *8*, e75913. https://doi.org/10.1371/journal.pone.0075913

Mai, J., Rao, C., Watt, J., Sun, X., Lin, C., Zhang, L., & Liu, J. (2019). *Mycobacterium tuberculosis* 6C sRNA binds multiple mRNA targets via C-rich loops independent of RNA chaperones. *Nucleic Acids Research*, *47*, 4292–4307. https://doi.org/10.1093/nar/gkz149

Mathews, D. H. (2006) RNA secondary structure analysis using RNAstructure. *Current protocols in bioinformatics*, *13*, 12.6.1–12.6.14. https://doi.org/10.1002/0471250953.bi1206s13

Miotto, P., Forti, F., Ambrosi, A., Pellin, D., Veiga, D. F., Balazsi, G., ... Cirillo, D. M. (2012). Genome-wide discovery of small RNAs in *Mycobacterium tuberculosis*. *PLoS ONE*, *7*, e51950. https://doi.org/10.1371/journal.pone.0051950

Mitra, A., Angamuthu, K., & Nagaraja, V. (2008). Genome-wide analysis of the intrinsic terminators of transcription across the genus Mycobacterium. *Tuberculosis (Edinb)*, *88*, 566–575. https://doi.org/10.1016/j.tube.2008.06.004

Mooney, R. A., & Landick, R. (2013). Building a better stop sign: Understanding the signals that terminate transcription. *Nature Methods*, *10*, 618–619. https://doi.org/10.1038/nmeth.2527

Moores, A., Riesco, A. B., Schwenk, S., & Arnvig, K. B. (2017). Expression, maturation and turnover of DrrS, an unusually stable, DosR regulated small RNA in *Mycobacterium tuberculosis*. *PLoS ONE*, *12*, e0174079. https://doi.org/10.1371/journal.pone.0174079

Morita, T., Ueda, M., Kubo, K., & Aiba, H. (2015). Insights into transcription termination of Hfq-binding sRNAs of *Escherichia coli* and characterization of readthrough products. *RNA*, *21*, 1490–1501. https://doi.org/10.1261/rna.051870.115

Mvubu, N. E., Pillay, B., Gamieldien, J., Bishai, W., & Pillay, M. (2016). Canonical pathways, networks and transcriptional factor regulation by clinical strains of *Mycobacterium tuberculosis* in pulmonary alveolar epithelial cells. *Tuberculosis (Edinb)*, *97*, 73–85. https://doi.org/10.1016/j.tube.2015.12.002

Namouchi, A., Gomez-Munoz, M., Frye, S. A., Moen, L. V., Rognes, T., Tonjum, T., & Balasingham, S. V. (2016). The *Mycobacterium tuberculosis* transcriptional landscape under genotoxic stress. *BMC Genomics*, *17*, 791. https://doi.org/10.1186/s12864-016-3132-1

Olejniczak, M., & Storz, G. (2017). ProQ/FinO-domain proteins: Another ubiquitous family of RNA matchmakers? *Molecular Microbiology*, *104*, 905–915. https://doi.org/10.1111/mmi.13679

Pelly, S., Bishai, W. R., & Lamichhane, G. (2012). A screen for non-coding RNA in *Mycobacterium tuberculosis* reveals a cAMP-responsive RNA that is expressed during infection. *Gene*, *500*, 85–92. https://doi.org/10.1016/j.gene.2012.03.044

Peters, J. M., Mooney, R. A., Kuan, P. F., Rowland, J. L., Keles, S., & Landick, R. (2009). Rho directs widespread termination of intragenic and stable RNA transcription. *Proceedings of the National Academy of Sciences of the United States of America*, *106*, 15406–15411. https://doi.org/10.1073/pnas.0903846106

Purkayastha, A., McCue, L. A., & McDonough, K. A. (2002). Identification of a *Mycobacterium tuberculosis* putative classical nitroreductase gene whose expression Is coregulated with that of the *acr* gene within macrophages, in standing versus shaking cultures, and under low oxygen conditions. *Infection and Immunity*, *70*, 1518–1529. https://doi.org/10.1128/IAI.70.3.1518-1529.2002

Rabhi, M., Espeli, O., Schwartz, A., Cayrol, B., Rahmouni, A. R., Arluison, V., & Boudvillain, M. (2011). The Sm-like RNA chaperone Hfq mediates transcription antitermination at Rho-dependent terminators. *EMBO Journal*, *30*, 2805–2816. https://doi.org/10.1038/emboj.2011.192

Ray-Soni, A., Bellecourt, M. J., & Landick, R. (2016). Mechanisms of bacterial transcription termination: All good things must end. *Annual Review of Biochemistry*, *85*, 319–347. https://doi.org/10.1146/annurev-biochem-060815-014844

Regnier, P., & Hajnsdorf, E. (2013). The interplay of Hfq, poly(A) polymerase I and exoribonucleases at the 3' ends of RNAs resulting from Rho-independent termination: A tentative model. *RNA Biology*, *10*, 602–609. https://doi.org/10.4161/rna.23664

Rudra, P., Prajapati, R. K., Banerjee, R., Sengupta, S., & Mukhopadhyay, J. (2015). Novel mechanism of gene regulation: The protein Rv1222 of *Mycobacterium tuberculosis* inhibits transcription by anchoring the RNA polymerase onto DNA. *Nucleic Acids Research*, *43*, 5855–5867.

Santangelo, T. J., & Artsimovitch, I. (2011). Termination and antitermination: RNA polymerase runs a stop sign. *Nature Reviews Microbiology*, *9*, 319–329.

Sassetti, C. M., Boyd, D. H., & Rubin, E. J. (2003). Genes required for mycobacterial growth defined by high density mutagenesis. *Molecular Microbiology*, *48*, 77–84. https://doi.org/10.1046/j.1365-2958.2003.03425.x

Sassetti, C. M., & Rubin, E. J. (2003). Genetic requirements for mycobacterial survival during infection. *Proceedings of the National Academy of Sciences of the United States of America*, *100*, 12989–12994. https://doi.org/10.1073/pnas.2134250100

Sato, K., Hamada, M., Asai, K., & Mituyama, T. (2009). CENTROIDFOLD: A web server for RNA secondary structure prediction. *Nucleic Acids Research*, *37*, W277–280. https://doi.org/10.1093/nar/gkp367

Sauer, E., & Weichenrieder, O. (2011). Structural basis for RNA 3'-end recognition by Hfq. *Proceedings of the National Academy of Sciences of the United States of America*, *108*, 13065–13070. https://doi.org/10.1073/pnas.1103420108

Schaefer, W. B., & Lewis, C. W. Jr (1965). Effect of oleic acid on growth and cell structure of mycobacteria. *Journal of Bacteriology*, *90*, 1438–1447.

Schnappinger, D., Ehrt, S., Voskuil, M. I., Liu, Y., Mangan, J. A., Monahan, I. M., ... Schoolnik, G. K. (2003). Transcriptional adaptation of *Mycobacterium tuberculosis* within macrophages: Insights into the phagosomal environment. *Journal of Experimental Medicine*, *198*, 693–704.

Schubert, O. T., Ludwig, C., Kogadeeva, M., Zimmermann, M., Rosenberger, G., Gengenbacher, M., ... Aebersold, R. (2015). Absolute proteome composition and dynamics during dormancy and resuscitation of *Mycobacterium tuberculosis*. *Cell Host & Microbe*, *18*, 96–108. https://doi.org/10.1016/j.chom.2015.06.001

Shi, L., Sohaskey, C. D., Kana, B. D., Dawes, S., North, R. J., Mizrahi, V., & Gennaro, M. L. (2005). Changes in energy metabolism of *Mycobacterium tuberculosis* in mouse lung and under in vitro conditions affecting aerobic respiration. *Proceedings of the National Academy of Sciences of the United States of America*, *102*, 15629–15634. https://doi.org/10.1073/pnas.0507850102

Shi, S., & Ehrt, S. (2006). Dihydrolipoamide acyltransferase is critical for *Mycobacterium tuberculosis* pathogenesis. *Infection and Immunity*, *74*, 56–63. https://doi.org/10.1128/IAI.74.1.56-63.2006

Shiflett, P. R., Taylor-McCabe, K. J., Michalczyk, R., "Pete" Silks, L. A., & Gupta, G. (2003). Structural studies on the hairpins at the 3′ untranslated region of an anthrax toxin gene. *Biochemistry*, *42*, 6078–6089.

Solans, L., Gonzalo-Asensio, J., Sala, C., Benjak, A., Uplekar, S., Rougemont, J., ... Cole, S. T. (2014). The PhoP-dependent ncRNA Mcr7 modulates the TAT secretion system in *Mycobacterium tuberculosis*. *PLoS Path*, *10*, e1004183. https://doi.org/10.1371/journal.ppat.1004183

Spalding, M. D., & Prigge, S. T. (2010). Lipoic acid metabolism in microbial pathogens. *Microbiology and Molecular Biology Reviews*, *74*, 200–228. https://doi.org/10.1128/MMBR.00008-10

Taverniti, V., Forti, F., Ghisotti, D., & Putzer, H. (2011). *Mycobacterium smegmatis* RNase J is a 5′-3′ exo-/endoribonuclease and both RNase J and RNase E are involved in ribosomal RNA maturation. *Molecular Microbiology*, *82*, 1260–1276. https://doi.org/10.1111/j.1365-2958.2011.07888.x

Tchigvintsev, A., Tchigvintsev, D., Flick, R., Popovic, A., Dong, A., Xu, X., ... Yakunin, A. F. (2013). Biochemical and structural studies of conserved Maf proteins revealed nucleotide pyrophosphatases with a preference for modified nucleotides. *Chemistry & Biology*, *20*, 1386–1398. https://doi.org/10.1016/j.chembiol.2013.09.011

Tjaden, B. (2008). TargetRNA: A tool for predicting targets of small RNA action in bacteria. *Nucleic Acids Research*, *36*, W109–W113. https://doi.org/10.1093/nar/gkn264

Tsai, C. H., Baranowski, C., Livny, J., McDonough, K. A., Wade, J. T., & Contreras, L. M. (2013). Identification of novel sRNAs in mycobacterial species. *PLoS ONE*, *8*, e79411. https://doi.org/10.1371/journal.pone.0079411

Uson, M. L., Ordonez, H., & Shuman, S. (2015). *Mycobacterium smegmatis* HelY Is an RNA-activated ATPase/dATPase and 3'-to-5' helicase that

unwinds 3'-tailed RNA duplexes and RNA:DNA hybrids. *Journal of Bacteriology*, *197*, 3057–3065. https://doi.org/10.1128/JB.00418-15

Vandal, O. H., Pierini, L. M., Schnappinger, D., Nathan, C. F., & Ehrt, S. (2008). A membrane protein preserves intrabacterial pH in intraphagosomal *Mycobacterium tuberculosis*. *Nature Medicine*, *14*, 849–854. https://doi.org/10.1038/nm.1795

Vasudeva-Rao, H. M., & McDonough, K. A. (2008). Expression of the Mycobacterium tuberculosis acr-coregulated genes from the DevR (DosR) regulon is controlled by multiple levels of regulation. *Infection and Immunity*, *76*, 2478–2489. https://doi.org/10.1128/IAI.01443-07

Venugopal, A., Bryk, R., Shi, S., Rhee, K., Rath, P., Schnappinger, D., … Nathan, C. (2011). Virulence of *Mycobacterium tuberculosis* depends on lipoamide dehydrogenase, a member of three multienzyme complexes. *Cell Host & Microbe*, *9*, 21–31. https://doi.org/10.1016/j.chom.2010.12.004

Waters, L. S., & Storz, G. (2009). Regulatory RNAs in bacteria. *Cell*, *136*, 615–628. https://doi.org/10.1016/j.cell.2009.01.043

WHO (2018). *Global tuberculosis report 2018*. Geneva: World Health Organization 2018.

Zadeh, J. N., Steenberg, C. D., Bois, J. S., Wolfe, B. R., Pierce, M. B., Khan, A. R., … Pierce, N. A. (2011). NUPACK: Analysis and design of nucleic acid systems. *Journal of Computational Chemistry*, *32*, 170–173. https://doi.org/10.1002/jcc.21596

Zeller, M. E., Csanadi, A., Miczak, A., Rose, T., Bizebard, T., & Kaberdin, V. R. (2007). Quaternary structure and biochemical properties of mycobacterial RNase E/G. *The Biochemical Journal*, *403*, 207–215. https://doi.org/10.1042/BJ20061530

Zhu, L., Phadtare, S., Nariya, H., Ouyang, M., Husson, R. N., & Inouye, M. (2008). The mRNA interferases, MazF-mt3 and MazF-mt7 from *Mycobacterium tuberculosis* target unique pentad sequences in single-stranded RNA. *Molecular Microbiology*, *69*, 559–569.

Zhu, L., Zhang, Y., Teh, J. S., Zhang, J., Connell, N., Rubin, H., & Inouye, M. (2006). Characterization of mRNA interferases from *Mycobacterium tuberculosis*. *Journal of Biological Chemistry*, *281*, 18638–18643.

Zuker, M. (2003). Mfold web server for nucleic acid folding and hybridization prediction. *Nucleic Acids Research*, *31*, 3406–3415. https://doi.org/10.1093/nar/gkg595

SUPPORTING INFORMATION

Additional supporting information may be found online in the Supporting Information section.